Historical floods of the Rhine river, reconstructed from the sedimentary fills of a dike breach pond and abandoned channels

Application for estimation of the design discharge

L.H.J. Aloserij BSc

Date: 05/10/2013

Dept. Physical Geography
Utrecht University
Supervision:
W.H.J. Toonen MSc
Prof. Dr H. Middelkoop

Summary

The low-lying Rhine Meuse delta is facing the risk of a disastrous flood. Such a flood could cause severe damage and losses to the Dutch population. To understand the risk of flooding, historical flood events are analyzed. For flood protection of the rivers in the Netherlands a data set of discharges is used to estimate the design discharge. The problem is that this discharge data set (~110 years, stored at *http://www.waterbase.nl)* is too short to precisely estimate the magnitude of a possible occurring flood with a recurrence time of 1250 years, the design discharge.

This study focuses on extending the discharge data set to decrease the uncertainty in estimation of extreme flood events. Investigating grain sizes in laminated deposits stored in dike breach ponds and abandoned channels helps to determine the magnitude of floods that have occurred in the past. Three coring locations were chosen for analysis. The locations represent the lower Rhine, Waal and Nederrijn (all three branches of the river Rhine). The three locations comply with the conditions demanded to answer the research question. All sites have well stored sediment and an unimpaired state. These are ideal circumstances for analysis of deposits from past floods.

The study shows the relationship between the P95 of the grain size distribution of flood deposits and associated discharges. It is possible to identify historical floods based on sedimentary layers in sediment fills of a dike breach pond and abandoned channels. Analysis of the sediment characteristics and the age depth curves are used to correlate the flood layers in the sediment fills to floods that occurred in historic time. A flood comparison of three locations gives insight in the impact of a historical flood at different locations.

The P95 value (sediment size) is connected to flood magnitude for the time frame 1817-2010AD. This discharge data set is extrapolated to the base of the three cores, around 1595AD. The discharge data with the expanded data is then used to calculate the return period and the design discharge of a once in 1250 year occurring flood. The maximum design discharge calculated, based on the converted discharge at Lobith (1817-2010AD) and the most extreme magnitudes of the three extrapolated data sets, is 15063 m^3/s for a once in 1250 year occurring flood. The current design discharge is set at 16000 m^3/s. The study concludes that this safety level is adequate for the present situation.

Table of contents

List of tables

List of figures

1	**Introduction**

The major flood of 1926 and the recently occurring floods near the Rhine and Meuse in 1993 and 1995 have shown the risk of a dike breach in the Netherlands. Dikes have to be strong enough to protect our society against floods by the Rhine and Meuse.

In the National Administrative Agreement on Water Affairs *(Dutch: "Bestuursakkoord Water")* the Dutch government, the provincial authorities, the municipalities, the district water boards, and the drinking water companies concluded that our population has to be secured against an extreme flood*.* A level of protection was determined with a return period of an extreme flood that statistically occurs once in 1250 years. This means that dikes have to be designed to resist a discharge with an annual probability of occurrence of 1/1250.

The design discharge (DD) is based on the maximal annual discharges of the last 110 years, which means a considerable uncertainty. The measured discharges series is too limited to determine a precise estimation of the design discharge magnitude.

Figure 1: The Rhine where it enters the Netherlands at Lobith (Google Earth, 2013)

Until 2000AD the design discharge for a possible occurring extreme flood was set at 15000 m^3/s. The climate is changing and with it more extreme discharges occur. Due to the floods in 1993 and 1995 the Dutch government decided to fix the design discharge in 2015AD, which the dikes need to be secured against in that year, at 16000 m^3/s.

The estimation of the design discharge has an uncertainty due to the limited data set; few data points in extreme reach. One extreme event can have a severe impact on the design discharge. To minimize the uncertainty a solution could be to use historical data of floods for a longer period. The Dutch stored data, some incomplete, of historic water levels in the Netherlands from 1770AD till the present. Besides the historical flood data, sediments were deposited in ponds and floodplains for thousands of years.

1.1	**Research objective**

The goal for this research is to reconstruct the magnitude and frequencies of historical floods at three different locations along the river Rhine. To achieve my goal the following research question has to be answered:

Is it possible to identify the magnitudes and recording times of historical floods (~1600 – 1900AD) based on sedimentary layers in sedimentary fills of dike breach ponds and abandoned channels in order to extend observed discharge records?

The sediment can be obtained till 1600AD. The laminated sediment layers characteristics combined with historical records and discharge data are used to obtain estimates for the discharge before the period, when the discharge (Q) is already known. Coring material from 3 different locations, which represent the full Rhine river and the Northern and Southern bifurcation after Lobith, give insight in the historical flood magnitude that occurred. The three sites are used to compare and determine the uncertainty in the estimates. The new data obtained in this study extend the data set of discharge measurements. This should result in decreasing the uncertainty of the expected extreme magnitude of a discharge with an annual probability of occurrence of 1/1250.

1.2	Study area

The study area is located around Lobith at the German-Dutch border (Fig. 2). Downstream of Lobith, the Rhine bifurcates into the Waal (Southern bifurcate) and the Nederrijn (Northern bifurcate). The distribution of the Rhine discharge over its lower distributaries Waal, Nederrijn-Lek and IJssel is governed by the channel morphology and the Pannerdensche Kop *(van de Ven, 1976)* at the bifurcation points. Since the end of the middle Ages, an increasing part of the Rhine water was carried by the Waal. The Pannerdensch Kanaal was dug to ensure a better water distribution and connected the Waal and the Nederrijn in 1707AD *(Middelkoop, 1997).* The building of dikes along the river branches was completed around the 13th century. The influence of these dikes was that the sedimentation in the floodplain almost disappeared. The channel migration decreased and focuses on a controlled embanked zone *(Hesselink, 2002)*. The only time sediment is deposited in the embanked floodplains is when a flood occurred, exceeding Q (~5000 m^3/sec) in the upper delta.

To study historical flood magnitudes of the Rhine, three coring locations were chosen. The coring points are located at a dike breach pond and an abandoned channel which are 'natural' sediment traps with a high preservation potential *(Toonen et al., 2012)*.

Figure 2: Study area (Google Earth, 2013)

Dike breach ponds
Dike breach ponds are formed during a dike breach. At the location of a dike breach, the water erodes a scour hole that can be over ten meters in depth. When the dike is rebuilt around the deep pond, the pond can become situated in the embanked floodplain area. Those ponds, situated within the embanked floodplain, have largely silted up: each time the floodplain inundates, river sediment enters these ponds *(Middelkoop, 1997)*.

The date of the dike breach that formed the pond can often be obtained from historical sources. Advantage is that the maximum period covered by the sediment layers is known. Sediments comprise the period of the strongest changes in the pollution of the Rhine river during the past 100-150 years (industrial revolution), which can help to determine the exact age of the existing sediment layers and to construct an initial age-depth model. Due to the unimpaired state of the pond it has a high preservation potential. Also due to the depth of the pond there is less bioturbation, which leads to perfect layering in the sediment cores.

Abandoned channels

Abandoned channels yield similar advantages as dike breach ponds. The age of channel abandonment can also be determined with the use of historical data, thus the age for the beginning of deposition. Most river sedimentation in an abandoned channel takes place during floods. This happens when the river water flows over the natural levee or over the secondary (summer bed) river dike towards the deposition point by exceeding a critical level for our study area (~5000 m^3/sec). Thus, the abandoned channels collect river sediment only in those years when the river water exceeds these critical levels. After the cut off, there is also a high preservation potential for the deposited layers *(Toonen et al., 2012)*.

1.2.1   Sample locations

In the study area three coring points are chosen (Fig. 2);

1. the 'Bienener Altrhein[1]' in a cut-off meander of the Rhine;
2. the 'Rijnstrangen[2]', an abandoned channel of the Nederrijn, the Northern branch;
3. the 'Zwarte Gat[3]', a dike-breach pond along the Waal, the Southern branch.

The three locations comply with the conditions demanded to answer the research question. Cores from these locations were available at the Utrecht University *(Table 1)*. The sediments at the different locations were obtained using a Livingston piston corer.

Table 1: Year that cores are obtained with the corresponding depth

Location	Obtained in (year)	Depth (cm)
1. Bienener Altrhein	2011	849
2. Rijnstrangen	2010	475
3. Zwarte Gat	1991	967

1.2.2   **Bienener Altrhein[1], Bienen (Germany)**

The 'full Rhine' core location is the Bienener Altrhein near Bienen. The Bienener Altrhein (BAR) is an old meander of the Rhine which became active in the 14th century *(Winkels, 2011)*. In the late 16th century, the Rhine shifted to the South-West (Grietherorther Altrhein). Here it stayed until the 18th century when the active channel was cut off and moved to the West. The location in the active floodplain and the close proximity of the Rhine's main channel to the abandoned BAR-meander means that the Rhine periodically floods the BAR-basin and introduces sediments. This resulted in a fast silting up of the channel. The BAR (Fig. 3) is an ideal location for reconstructing the magnitude of historical floods based on sedimentary characteristics of the channel fill, because active sedimentation still takes place. This means that the sediment core is most likely to show an overlap with the discharge dataset of the last ~240 years *(Toonen et al., in prep)*.

Figure 3: Core location 1. Bienener Altrhein, Germany (Google Earth, 2013)

1.2.3   **Rijnstrangen[2], Pannerden (the Netherlands)**

The second coring point is located in a sharp bend of the Rijnstrangen, North of Pannerden (Fig. 4). The residual channel marks the historical right hand Nederrijn bifurcation channel of the Rhine *(Kleinhans et al., 2011)*. Around 1600AD, the Rijnstrangen (RSTR) had lost almost all discharge to the Waal, by natural changes of the course of the Rhine river, which disconnected the RSTR bifurcation channel during the 16th and 17th century. In 1707AD the Pannerdensch Kanaal was completed, which cut off the Rijnstrangen branch. Until 1959AD waters remained to be directed into the RSTR residual channel, during larger floods *(Toonen et al., 2012)*. Currently, the RSTR channel carries local drainage. Upstream the Pannerdensch Kanaal is connected to the Rijnstrangen through groundwater exchange. Due to disconnection of the Rhine the location has a high preservation potential.
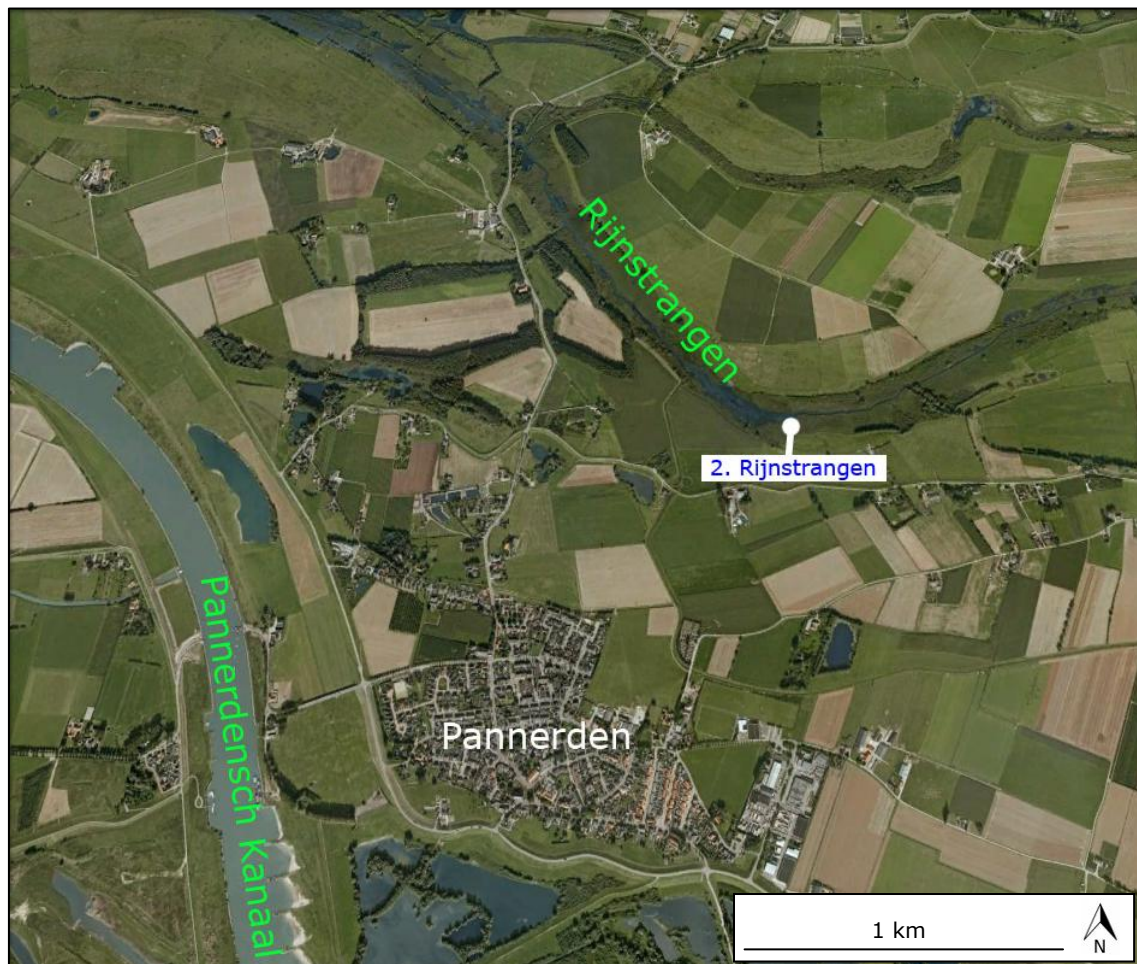
Figure 4: Core location 2. Rijnstrangen, the Netherlands (Google Earth, 2013)

1.2.4   Zwarte Gat[3], Slijk-Ewijk (the Netherlands)

The pond called Zwarte Gat (Fig. 5) formed in 1644AD near Slijk-Ewijk *(Middelkoop, 1997),* due to a dike breach caused by seepage. The coring location is located at the Northern side of the Waal. Deposition in the pond occurred each time the water level in the Waal reaches high enough to flood the pond. The sedimentation rate (without compaction) in the Zwarte Gat pond is about 1.4 cm/year *(Middelkoop, 1997).* The minimal entrance and disturbance of sediment and water into the pond gives a high preservation potential which is necessary for good results. The sediment in the pond exists of mainly suspended load.

Figure 5: Core location 3. Zwarte Gat, the Netherlands (Google Earth, 2013)

2	Methods

2.1	General approach

2.1.1   Sediment analysis

Sediments are deposited in the ponds and abandoned channels with each flood that overflows the embankment. Every flood moves different sizes of sediment related to the magnitude of the flood. The greater the flood, the more coarse sediment is transported. Therefore sediments contain information about the size of floods. During this research the sediments were analyzed.

2.1.2   Discharge

The connection between discharge and the coarseness of sediment was examined. Floods occur when the river water level exceeds the embankment. The discharge of these floods determines the impact. To minimize the impact of floods a prediction of the highest possibly occurring flood was determined. With this knowledge the embankments strength can be increased to withstand a flood in the future.

2.1.3   Historical records

Historical records can be used to indicate the magnitude of a specific flood at the year it occurred. The records that are used consist out of the converted Q at Lobith, the water level data of Cologne and the number of dike breaches that occurred. The Buisman series contains a collection of different historical records regarding to meteorological events. The dike breaches come out of the Buisman series and have been stored from 750AD till the present *(Buisman series: "Duizend jaar wind en water in de Lage Landen")*.

2.2	Laboratory analysis

In the laboratory, the sediment cores were split along the longer axis into two halves. The sections were photographed and then described. The description was done by logging the following information:

1   The upper and lower boundaries of the described cores.
2   Lithological units based on the structure, texture.
3   Color of the sediment related to interlaying with other types of sediment.
4   Bioturbation, sedimentary clasts, pebbles, shells, etc.
5   Disturbances due to the coring operation and/or transportation.

To define the amount and type of deposition during a flood, organic content (loss on ignition) and sediment coarseness (grain size) were determined.

2.2.1   Organic content

The organic content is measured for sedimentation rates. The LOI method is used to measure the weight percentage of organic matter in sediments. The protocol is described by Heiri et al. *(2001)*. Samples of 1 cm intervals of a constant volume were taken. The presence of more clastic material during flood events will reduce the relative contribution of organic material in a sample. Therefore, a flood event will be indicated with a decrease in volume of organic material in LOI.

In the laboratory, samples were put in open tubes and their bulk weight was measured. The weight of the tube, measured beforehand, is subtracted to obtain the sample bulk weight. The samples were dried before sample dry weight was determined again. Difference is the samples water content, which is assumed to be responsible for the total of weight loss during this stage. After drying, samples were placed in a stove and heated for 5 hours to 550 ºC. After cooling the batch was removed from the stove and the remaining samples were weighed. The weight loss of the sample is attributed to combustion of organic carbon during ignition time in the stove and the reaction of CaCO3 in small amounts. The difference between sample dry weight and final weight is divided by the sample's dry weight to obtain a weight percentage of organic matter; the loss on ignition percentage.

2.2.1   Grain size analysis

The sediment grain size gives an estimation of the magnitude of the historical flood. A higher magnitude flood can transport larger grains than lower magnitude floods *(Winkels, 2011)*. Two cm interval samples, related to visual layering and adjusted, were taken for the detailed grain size analysis.

Before starting the samples processing (done by using a Laser Particle Sizer) organic matter, carbonates and CA^2+ and FE^3+ ions were removed. The samples were treated with a 30% H_2O_2 solution which eliminates all the organic material. Then a 10% HCL solution eliminated all carbonates. The Ca^2+ and FE^3+ ions were removed with 300 mg of natriumpyrophosphat which also splits the electorally charged particles to prevent particles to merge. Grainsize details were determined at the VU (Amsterdam) using a Laser Particle Sizer.

The two parameters used for identification and qualification of the different flood layers are the sand percentage and the 95th percentile (P95) value. The P95 describes the size of the 5% largest particles in each sample.

2.3	**Sedimentary layers vs. historical records**

The following steps were taken to answer the research question:

At every location

1. The LOI, sand and P95 values were analyzed at 2 cm intervals to identify sediment layers deposited during major flood events. The coring samples are divided into sections. The sections are based on the percentage of sand and the P95. During recovery the core material was slightly compressed. Therefore the data shows gaps. The assumption is made that gaps are a result of the drilling, which compressed the material and no material is lost. To stretch the core depths, the top of the individual coring samples are connected to the bottom depth of the higher coring sample above. The stretch calculation gives the true core depths.

2. Calculation of an age depth curve, by using available historical flood magnitudes information, to estimate the year a layer was deposited.

3. Flood reconstruction based on the correlation of the highest peak values in P95 with the known data was applied to correct the age depth curve. Every correlation corrects the age depth curve and makes estimations more accurate.

Comparison

4. In order to detect the same flood event in all three cores they need to be compared. Different sediment characteristics occurred at every location due to the impact of the flood and the composition of the sediment. To compare the locations, the P95 values were normalized. The deviation of all normalized P95 values in each section of the cores shows a trend of the correlated discharge. This trend is an estimation of the development of magnitude of a possibly occurring flood. These discharges were compared.

5. The age depth curve was corrected by indentifying the same pattern in the occurring peaks after normalization among the three cores and correlating them with the historical floods. For example: if a flood occurred in the normalized graphs at the Zwarte Gat and BAR core at 1700AD and at the Rijnstrangen a peak can be seen at 1699AD then the Rijnstrangen peak is fixed at 1700AD.

Discharge

6. Defining discharges based on sediment layers was done by a correlation of the calibrated age/depth – P95 correlation against the converted and registered Q Lobith for 1817-2010AD. The normalized P95 values correlated peaks in this period for each location were determined by plotting them into a graph to define the trend. The trends contain an uncertainty which depends on the scattering of extreme values. The trend for the period 1817-2010AD was used for the extrapolation of the samples back to 1595AD.

Application

7. For the three locations the return period of the extreme floods and the design discharge was calculated. Also the most extreme situation (largest discharge of the three location based cores) was used to define the return period. This extreme situation contains all of the known and correlated floods and therefore it was used to estimate the maximal design discharge.

3			Results

3.1			Sedimentary characteristics

3.1.1   Bienener Altrhein

Table 2: Bienener Altrhein core description

Section	Depth (cm)		Description trends and peaks	Peak values at (cm)		Sand (%)	P95 (µm)
1 **2-91**		2-12	Low values of sand percentage and P95 content.		Max. Min.	6.8 1.4	78 43
Top layer. Coarse sand.		12-60	High sand content and P95.		Max. Min.	73.3 23.4	589 317
		60-91	Upward increase of sand and P95.		Max. Min.	24.6 4.4	277 60
2 **93-151**			A gradually upward increase of sand and P95.		Max. Min.	18.0 3.3	138 55
Rise in sand content.			Coarse peaks.	103 110		16.4 14.6	138 127
3 **153-842**			A persistent trend in sand and P95 values.		Max. Min.	50.4 0.03	209 26
Stable laminated. Silty clay.			Corresponding peaks in sand percentage and P95 content.	155 239 276 333 358		15.1 15.8 13.7 7.4 7.2	131 179 135 77 79
			Compared to the trend line larger peaks occur at these depths.	446 564		12.6 8.5	109 76
			The most striking peaks in a small range for sand and P95.	659 683		50.4 7.6	209 112
			First two spikes that are noticed after the scour hole emerged.	822 833		8.5 9.2	103 174
4 **844-849**			The abandoned channel base is reached.	849		32.9	706

Organic content

For the Bienener Altrhein the loss on ignition (Fig. 6) values range between 4 and 8%, with average 5.7%. From 2 cm till 91 cm there is a wider range of organic matter content and also the sand and P95 percentages are high. This is probably caused due to the excavation and filling up of sand during the building of a sluice in 1920AD *(Bunnik, pers. comm.)*.

Sand percentage and P95 value

The sand (Fig. 6) and P95 graphs show similar of peaks. High sand and P95 amounts coincide with low organic matter contents. This can also be seen at 659 cm where a large peak in the sand and P95 content corresponds to a low LOI value. Apparently at this specific moment a large flood occurred that contained a large amount of clastic material. The trends in sand and P95 values are described in table 2.
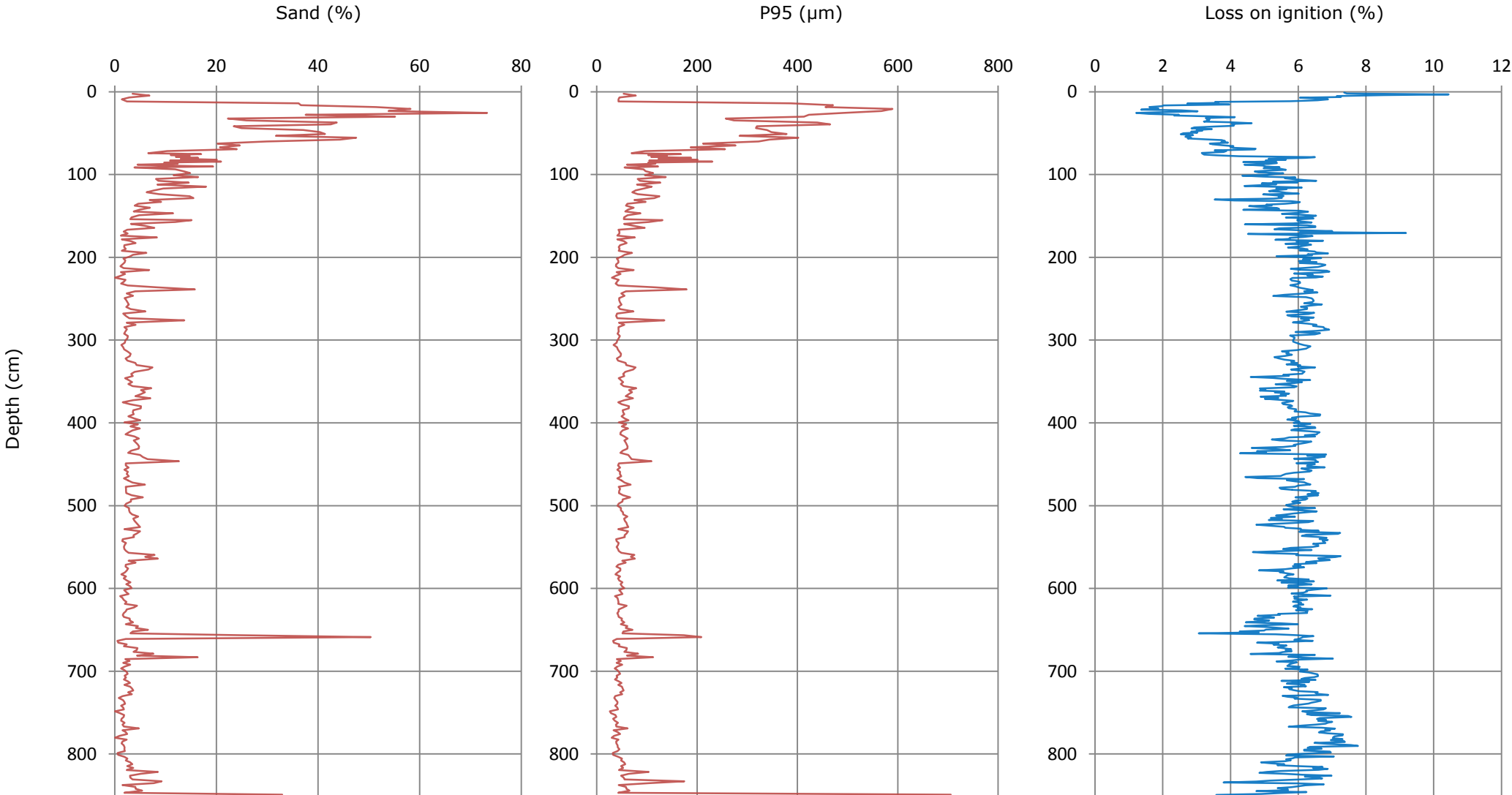
Figure 6: Bienener Altrhein: sand percentages, P95 values and loss on ignition percentages.

3.1.2 Rijnstrangen

Table 3: Rijnstrangen core description

Section	Depth (cm)		Description trends and peaks	Peak values at (cm)		Sand (%)	P95 (µm)
1	**5-110**		Four spikes can be noticed in this section. The four spikes can be split into 2 parts due to the difference in P95 content.		Max. Min.	84.4 7.6	805 91
		5-60		33 52		84.4 78.8	389 307
		60-110		70 83		67.8 61.8	681 805
2	**114-257**		Gradually increase of sand and P95. Highest peak for sand:	222 238	Max. Min.	68.4 4.6 60.6 68.4	281 61 297 281
3	**258-455**		Continuous trend for sand and P95 in the graph.		Max. Min.	43.7 3.3	201 51
		258-295	Slowly decrease of sand and P95 content. Peak can be seen:	269	Max. Min.	37.7 7.3 37.7	178 74 178
		295-347	Low range and change for sand and P95.		Max. Min.	25.1 3.3	154 51
		347-413	Increase that results in 3 major peaks:	359 373 383	Max. Min.	43.7 5.2 43.7 29.9 22.7	201 65 173 156 201
		413-455	Continuous values for sand and P95, with an increase at 443 cm resulting in a peak.	443	Max. Min.	28.6 5.0 28.6	170 63 170
4	**457-475**		After the emergence of the scour hole the number of sand and P95 is extremely high.		Max. Min.	96.8 6.1	1133 75

Organic content

The average loss on ignition percentage for the whole core is 5.6% (Fig. 7). The striking peak at 178 cm depth has a percentage of 24.9%. The organic matter content between the depth ranges from 174 till 182 cm has an average of 12.2%. The peak of 24.9% cannot be linked to a depth in the sand and P95 graph.

Sand percentage and P95 value

Both the sand and P95 (Fig. 7) lines show similar peaks. The more sand present in a sample the greater the size of the largest particle. The sand percentage in the Rijnstrangen is higher than the sand percentage in the BAR sediments. This can be dedicated to the setting of the coring points. In comparison with the BAR location, more sandy material was deposited during historical floods at the Rijnstrangen point. The peaks and trends in sand and P95 values are described in table 3.
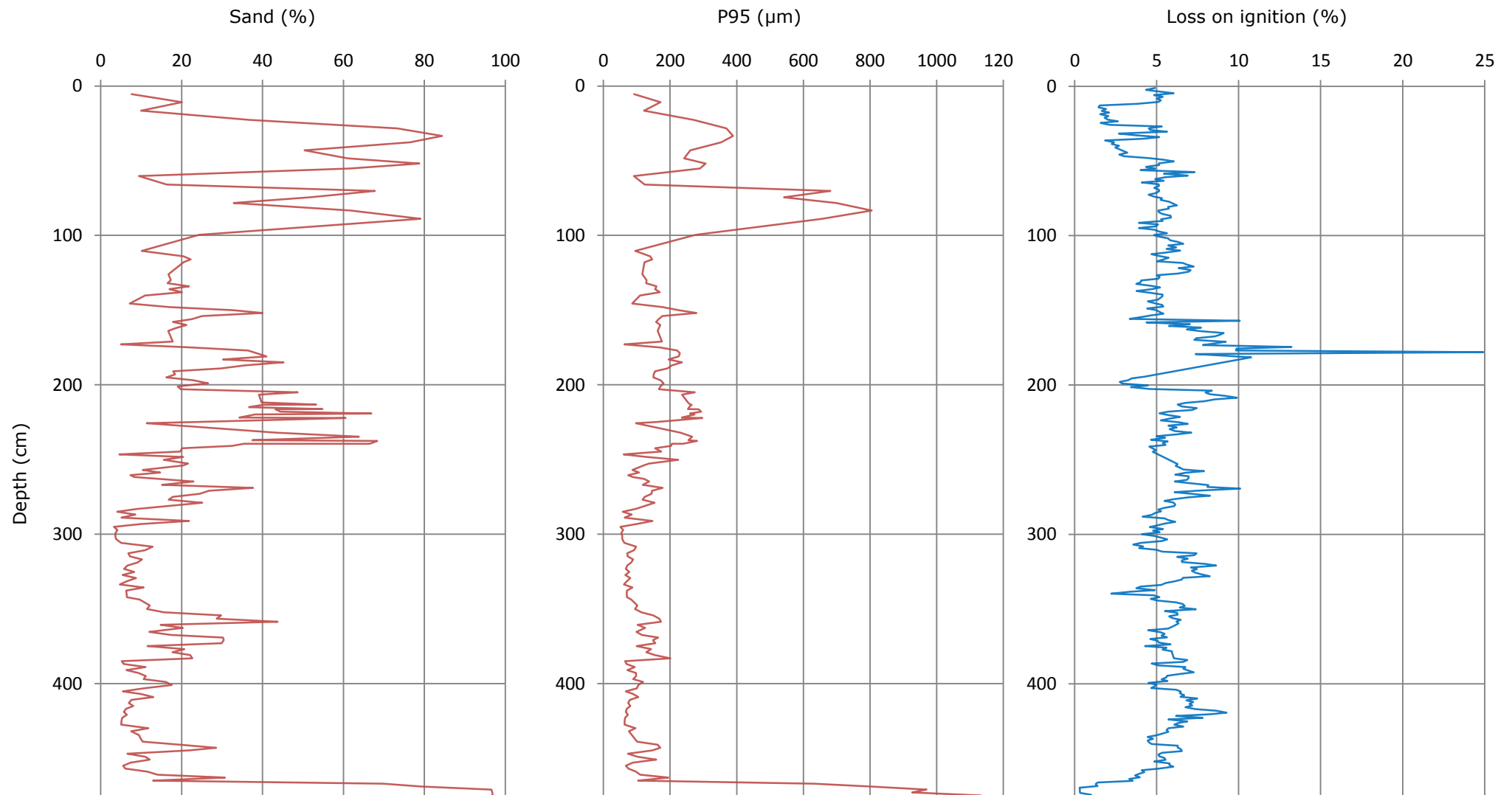
Figure 7: Rijnstrangen: sand percentages, P95 values and loss on ignition percentages.

3.1.3   Zwarte Gat

The Zwarte Gat core can be divided in 4 sections. Table 3 describes the sections. The top of the core starts at 30 cm depth below surface due to the presence of water and/or unconsolidated material.

Table 4: Zwarte Gat core description

Section	Depth (cm)		Description trends and peaks	Peak values at (cm)		Sand (%)	P95 (µm)
1	**30-253**		Continuous trend in sand and P95 percentages.		Max. Min.	13.4 1.2	132 34
		30-123	4 peaks for sand and P95.	32 60 90 123		8.7 7.3 6.5 9.2	116 98 77 130
		123-253	A gradually increase in sand and P95 values.	164 188 245		6.0 13.4 7.8	72 132 88
2	**254-453**		Continuous trend with a high range in sand and P95.	287 314 358 380 434	Max. Min.	21.9 1.5 21.9 6.6 8.9 10.7 6.4	370 37 370 74 78 88 69
3	**456-693**		A small peak followed by an increased percentage of sand and P95 content.	488 582	Max. Min.	7.4 0.03 5.3 7.4	77 28 65 77
4	**698-967** At this depth the Zwarte Gat was positioned closer to the Waal		Higher percentages of sand and P95 values. Around 16% for sand and 118 µm for P95 five peaks are noticed. Highest peak at:	712 770 777 795 829 868	Max. Min.	25.6 1.6 16.5 15.9 16.2 16.0 16.4 25.6	137 43 121 127 119 111 113 137

Organic content

The LOI values are available till 569 cm depth. The LOI graph (Fig. 8) shows after 100 cm depth a value between 5 and 8%. The peak at 45 cm is not connectable to corresponding low values for sand or P95.

Sand percentage and P95 value

The contours of sand and P95 are similar in both graphs (Fig. 8). The trends in sand percentage and P95 values for the Zwarte Gat are described in table 3. Compared to the other locations the Zwarte Gat contains less sand. Overall the largest particle sizes are below 100 µm. One large peak is noticed at 287 cm with a sand percentage of 21.91% and a P95 value of 369.7 µm. These peaks cannot be linked to an extreme LOI value at the same depth.
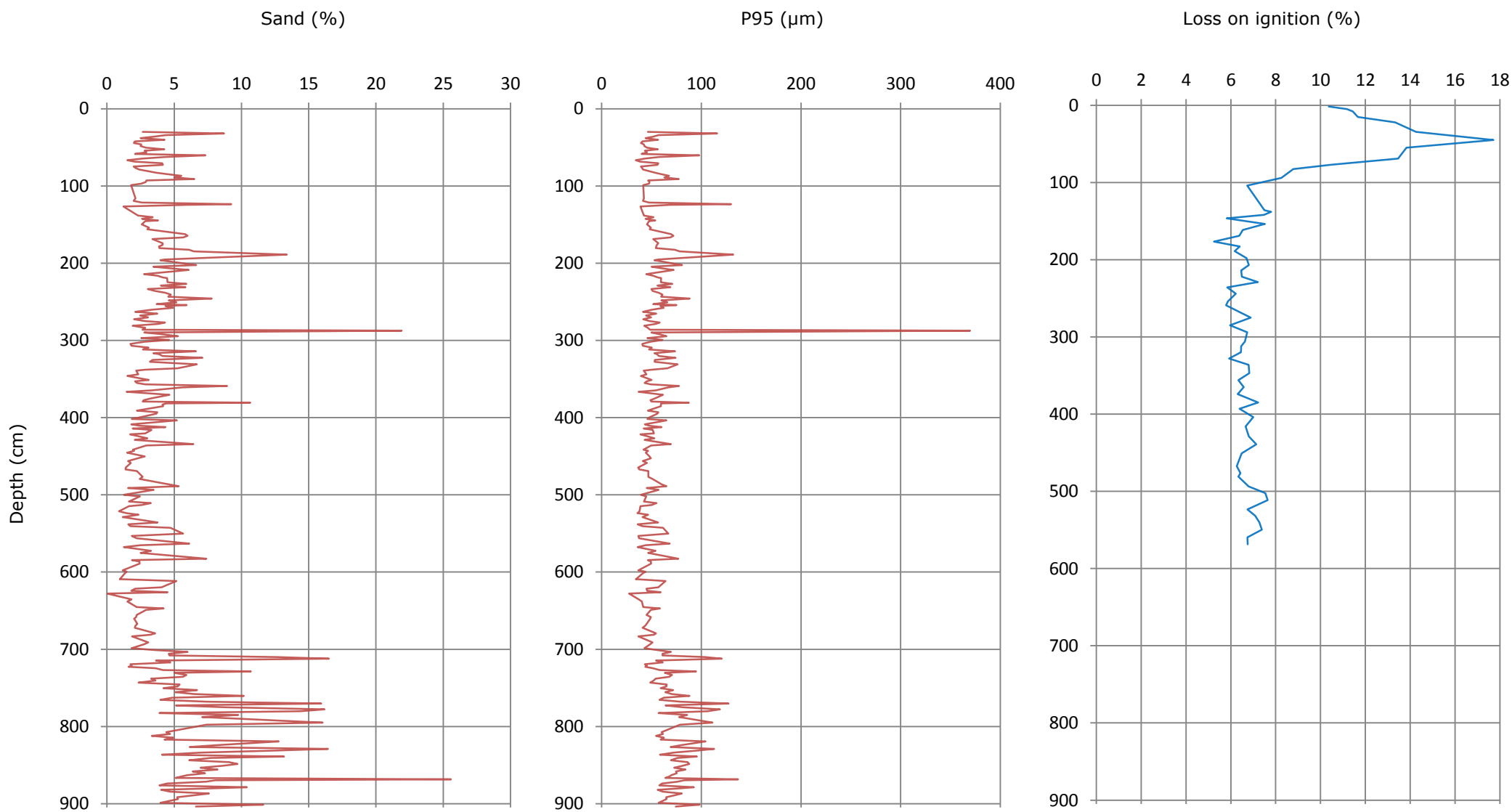
Figure 8: Zwarte Gat: sand percentages, P95 values and loss on ignition percentages.

3.2	**Age depth curves**

Age depth curves show the relationship between the core layers and the estimated year of deposition. The known information for the three locations results in the following age depth curves (Fig. 9).
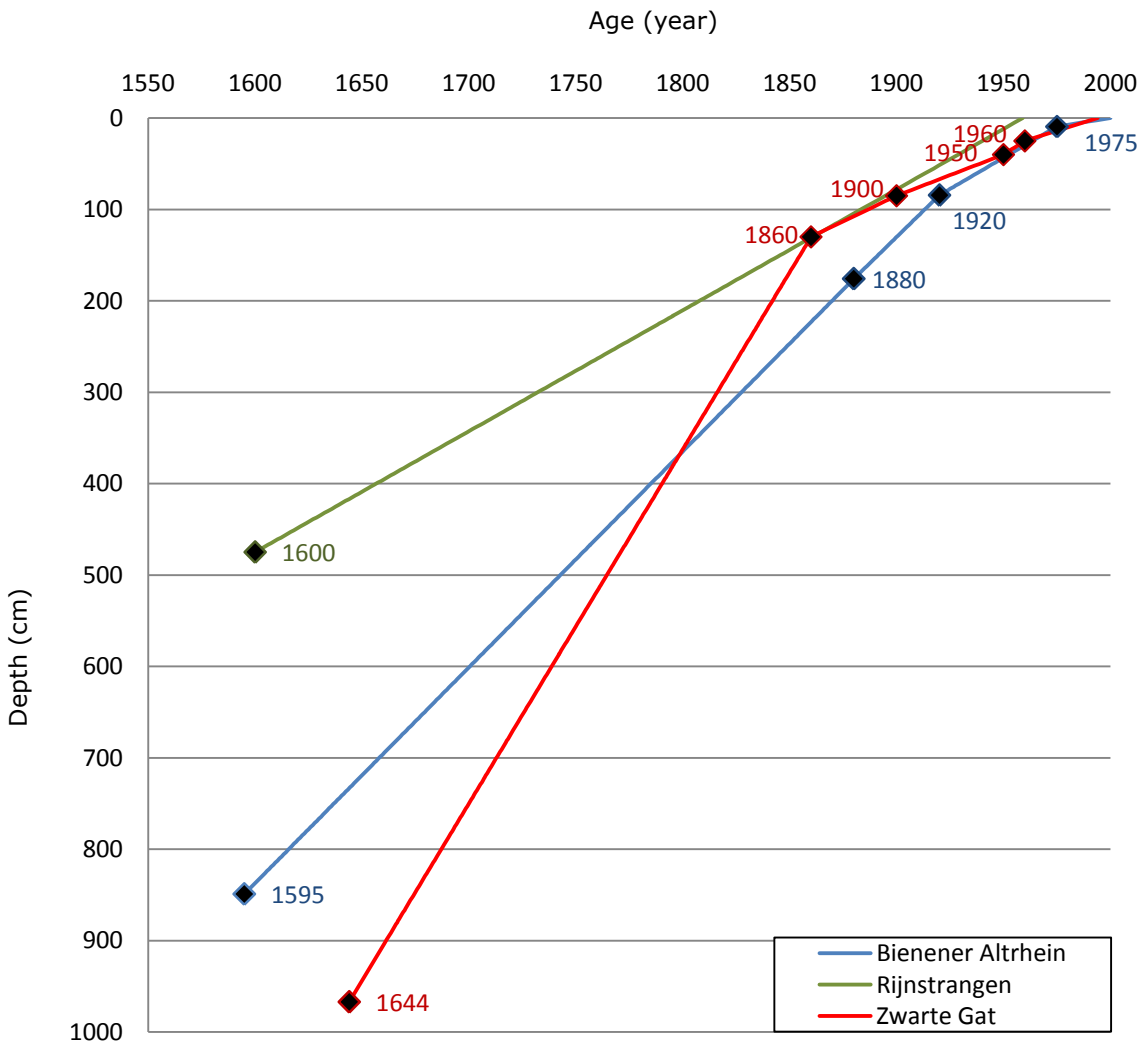
Figure 9: Initial age depth curves for the three coring locations

Bienener Altrhein

The abandonment of the BAR can be traced back to the period 1550-1600AD *(Winkels, 2011)*. Its origin is presumably the big flood that occurred at 1595AD. The large peak in sand located at 84 cm (Fig. 6) is attributed to the construction of a sluice in 1920AD *(Bunnik, pers. comm.)*. Palynological analysis done by TNO suggests an age between 1900-1975AD at 10 cm depth (no hemp, maize, much rye, pine). The same analysis indicates that at 174 cm depth the pollen obtained much hemp and buckwheat. This sets this depth at being older than 1880AD, due to the non presence after 1880AD of hemp and buckwheat. The known top age is 2010AD. The blue line in figure 4 shows the age depth curve for the Bienener Altrhein.

Rijnstrangen

The age knowledge of the core of the Rijnstrangen is rather limited. Around 1600AD it lost almost all discharge to the Waal *(Kleinhans et al., 2011)*. The channel continued to silt up even after the closure in 1950AD till 1959AD *(Steenhouwer et al., 2005)*. After 1959AD river sediment or organic material could have entered the channel. It is assumed that this has not taken place. The know knowledge leads to a bottom age of 1600AD and a top age of 1959AD. The age depth curve is shown with the green line in figure 4.

Zwarte Gat

The pond his origin is around 1644AD *(Middelkoop, 1997)*. The core was taken in 1994AD. This gives a bottom age of 1644AD and a top age of 1994AD for the Zwarte Gat core. Middelkoop (1997) correlated heavy metal contents with the sediments age (Table 5). The years in the blue boxes can be fixed in the age depth curve to give an indication of the age. The green boxes give an indication that can help with the flood reconstruction by using the period correlations as a check to the age depth curve. With the known information the red age depth curve was established (Fig. 9).

Table 5: Correlations of heavy metal contents and sediments year of origin (Middelkoop, 1997)

Depth (cm)	Cu (mg/kg)	Pb (mg/kg)	Zn (mg/kg)	Period (year)
25	140-160	180-220	800-950	Around 1960AD
40				Around 1950AD
40-50	50-70	100-130	650	Late 1930s
50-85	150	300-450	1150-1550	Mid 1930s
85	40-70	140-180	500-600	Around 1900AD
130				Around 1860AD
150-200	20-30	60-80	150-180	Around 1850AD

3.3	Flood magnitude reconstruction

Peak values in the P95 and sand percentage were used for identification of flood laminations in the different cores. Correlating the peak values to known historical floods was done with the age depth curves. The curves are a guideline for the estimation of the floods layers year of origin. Based on the limited age control, it is impossible to precisely connect the P95 and sand values to historical floods. First the highest peaks in P95 content are correlated followed by the upcoming lower peaks over the entire depth of the core. In this order the floods ages are connected and introduced as tie-points into the age depth curve for further correlation till the most pronounced floods are linked.

Historical flood magnitudes (App. 1) are indicated by the number of dike breaches that occurred along the lower Rhine branches during a single flood, water levels at Cologne (1901-2010AD) and the discharge estimations at Lobith of historical records. Table 6 represents the classes that divide the known data. The largest floods are assigned to class 1. Class 2 till 5 represent smaller floods divided in that order. The discharge estimations at Lobith are based on a calibration done by Toonen et al. *(in prep.)* using annual peak discharges at Cologne for the period 1901-2010AD. Regression provided the estimation for the period 1817-2010AD. The classes are used for the impact classification of the historical floods.

Table 6: Class distribution of the historical floods impact

Classes	Breaches	Waterlevel (m) + historical records Köln	Estimated Q Lobith (1817AD-2010AD)
1	>10	>13 m	>13000 m^3/s
2	5-10	11-13 m	11000-13000 m^3/s
3	2-4	10-11 m + major flood	10000-11000 m^3/s
4	1	9-10 m	9000-10000 m^3/s
5	0	<9 m	<9000 m^3/s

The tables 7, 8 and 9 show the correlation between depths and historical floods for the three locations. The highest P95 values are correlated to the floods with the highest water level or discharge. The first direct connections are indicated by the red boxes. The green boxes represent the secondly made estimated connections. The column 'Estimated AD' shows the estimated year with added additional benchmarks in the age depth curve.

3.3.1   **Bienener Altrhein**

The bottom of the core gives the largest P95 value due to the presence of gravel at the channel base. The age depth curve estimates the year 1930 at the depth of 69 cm. In the year 1920AD a sluice was constructed that had a disruptive influence on the sediments after 1930AD. Therefore the depth till 69 cm is not taken into account. The building of the sluice coincided with the flood of 1920AD therefore this flood is not taken into account.

The peak that really stands out is at 659 cm. This peak is related to the year 1675AD according to the age depth curve. However, the largest flood during this period occurred in 1682AD which was therefore linked to 659 cm. The adjustment to the age depth curve estimates the 2 peaks at 239 cm and 276 cm at 1853AD and 1838AD respectively. Around this period 2 major floods with a water level of more than 10 m occurred, 1850AD and 1845AD. Both of these floods were therefore connected to the corresponding depths. The same technique was used for the peaks at 155 cm and 164 cm. The estimated year of the laminations origin connects the depths to the floods of 1883AD and 1882AD. The floods in table 6 were estimated, correlated and linked to the corresponding P95 values at the different depths.

Figure 10 shows the sand percentage and P95 value at the Bienener Altrhein correlated to the years the historical floods occurred and refined age-depth model.

Table 7: Historical flood correlation Bienener Altrhein

Depth (cm)	Sand (%)	P95 (µm)	Initial age-depth model (year AD)	Historical flood age (year AD)
5	7	78		
21	58	589		
39	43	465		
51	41	378		
56	48	402		
69	24	256	1930	1930
75	17	168	1926	1926
80	16	188	1922	1924
155	15	131	1888	1883
164	8	96	1882	1882
183	4	59	1876	1876
215	7	74	1860	1862
227	2	44	1855	1855
239	16	179	1853	1850
276	14	135	1838	1845
333	7	77	1820	1820
446	13	109	1770	1784
475	6	68	1767	1770
490	6	67	1763	1758
513	5	61	1752	1753
526	5	63	1746	1747
531	5	63	1743	1744
538	4	56	1740	1741
559	8	75	1730	1729
564	9	76	1727	1726
585	2	47	1717	1716
593	3	51	1714	1711
600	3	55	1710	1709
621	4	60	1700	1699
637	3	50	1693	1694
659	50	209	1675	1682
683	16	112	1671	1671
714	3	49	1656	1658
723	4	54	1652	1651
737	2	41	1646	1644
746	2	42	1642	1638
755	2	39	1638	1635
762	2	42	1635	1634
783	2	43	1625	1624
794	2	45	1620	1618
812	4	57	1611	1609
822	9	103	1607	1608
833	9	174	1602	1602
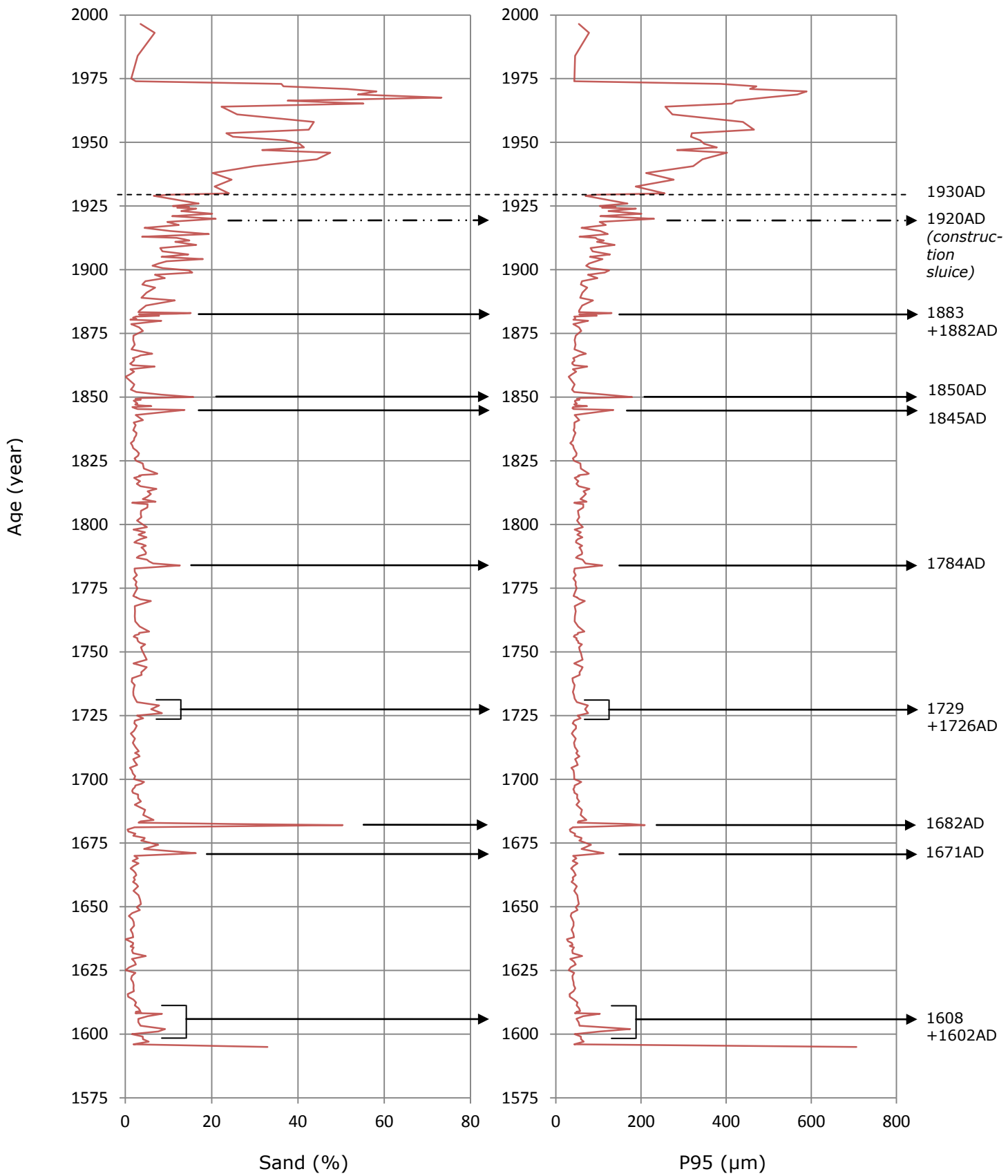
Figure 10: Bienener Altrhein flood reconstruction sand percentage and P95

3.3.2   Rijnstrangen

The Rijnstrangen P95 data shows a large peak at 83 cm. With the age depth curve this depth has an estimated age of 1896AD. Before this large peak another peak occurs at 70 cm which is estimated at 1906AD. Both high peaks, within an estimation of 10 years time difference, lead to the floods of 1920AD (11365 m^3/s) and 1926AD (13000 m^3/s) *(Toonen et al., in prep)* (Fig. 11). After determination of the laminations origin of these 2 peaks, the other extreme values have been connected in order of P95 size with the highest occurring water levels (Table 6). Table 8 is the result of every correlation that is made using this method.

AMS (accelerator mass spectrometry) dating determined that at 2.07 - 2.10 meters below the ground surface the year of origin is around 1870AD (+/- 69 years). In the table the depth of 205 cm is connected to the flood of 1820. This corresponds reasonably well to the AMS dating.

Figure 11 shows the sand percentages and P95 values at the Rijnstrangen connected to the years the historical floods occurred.

Table 8: Historical flood correlation Rijnstrangen

Depth (cm)	Sand (%)	P95 (µm)	Initial age-depth model (year AD)	Historical flood age (year AD)
11	20	171	1955	1955
33	84	389	1943	1948
52	79	307	1937	1930
70	68	681	1906	1926
83	62	805	1896	1920
130	17	130	1883	1883
134	22	159	1879	1882
138	20	169	1875	1876
152	40	279	1868	1862
160	21	171	1856	1855
171	18	175	1847	1850
179	39	230	1841	1845
185	45	236	1836	1833
199	27	181	1825	1824
205	49	274	1823	1820
213	40	265	1816	1819
218	44	293	1812	1814
222	61	297	1810	1809
235	64	266	1798	1799
238	68	281	1796	1795
250	16	225	1785	1784
269	38	178	1770	1770
279	25	154	1762	1758
291	22	147	1749	1753
308	13	98	1740	1741
348	12	102	1708	1709
359	44	173	1701	1699
369	30	165	1697	1694
383	23	201	1675	1682
389	11	94	1677	1677
399	16	119	1667	1671
409	13	105	1657	1658
415	8	80	1652	1651
421	7	74	1646	1644
430	12	96	1637	1638
443	29	170	1628	1624
451	12	158	1618	1618
463	31	195	1609	1609
471	97	970	1603	1602

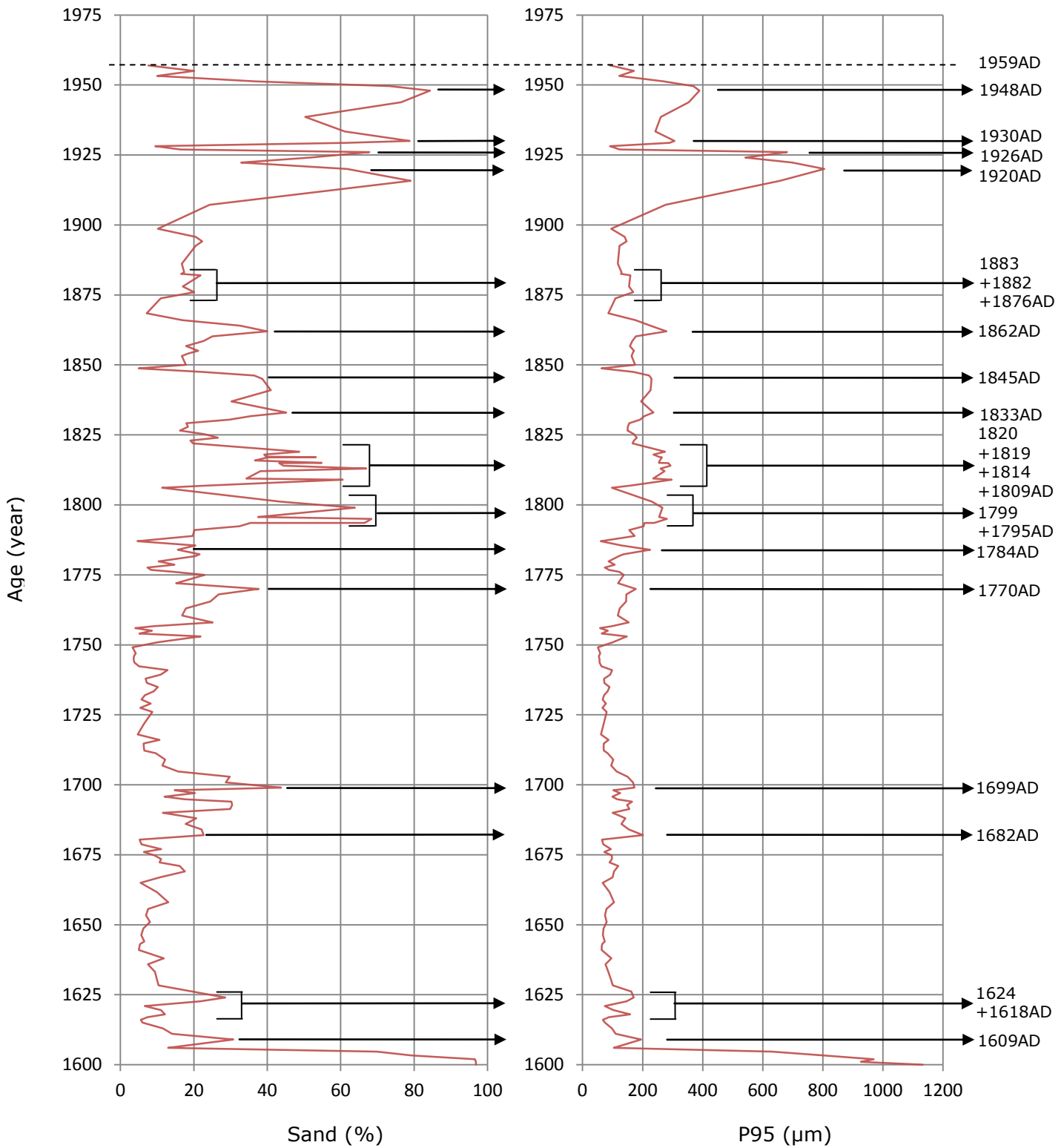*Figure 11: Rijnstrangen flood reconstruction sand percentage and P95*

3.3.3   Zwarte Gat

The top age of the first peak at 32 cm is set at the flood of 1955AD. Correlations of heavy metal contents and sediments year of origin done by Middelkoop (1997) indicates this flood because its origin is between 1950 and 1960AD.

The initial age-depth model shows three peaks between 85 cm (~1900AD) and 130 cm (~1860AD) depth. These peaks are initially estimated at 1898AD, 1895AD and 1866AD. The high P95 values can be linked to the floods of 1883AD, 1882AD and 1862AD (App. 1). The assumption was made that due to the age depth correlation and the gap, missing sediment layers, between 99 cm and 116 cm that the flood of 1876AD is located in this period.

These fixed ages reset the age depth relationship for further correlations. The highest extreme P95 value between 1950AD (~40cm depth) and 1900AD (~85cm depth) with a value of 98 µm can be seen at 60 cm depth. With the extra information of the correlations (Table 5) made by Middelkoop *(1997)* the age of the laminated sediment should be in the mid-1930s. The estimated age of 1927AD correlates this depth with the historical flood in 1926AD.

The largest major peak can be seen in the P95 data of the Zwarte Gat at 287 cm, with 370 µm. The estimated age lies around 1819AD. The highest water levels near this year are the large floods of 1819AD and 1820AD. At 1819AD a water level was measured at 9.63 m in Cologne and in 1820AD the water level was 9.40 m in Cologne. The 1820AD high water caused more dike breaches which led to more coarse sediment. Therefore this peak is set at 1820AD.

The other less pronounced flood layers show few differences over a large range. The highest values in P95 are used again to maintain the logical sequence; starting the correlation from large P95 values downwards until low P95 values. Table 9 gives a summary of the linked age to the different lamination depths. One added check can be made at 3 peaks with the estimated ages of 1851AD, 1849AD and 1845AD. The depth of these peaks lies between 150cm and 200cm, exactly in agreement with the metal contents ages determined by Middelkoop *(1997).*

The sand percentages and P95 values at the Zwarte Gat connected to the years the historical floods occurred are displayed in figure 12.

Table 9: Historical flood correlation Zwarte Gat

| Depth (cm)	Sand (%)	P95 (µm)	Initial age-depth model (year AD)	Historical flood age (year AD)
32	9	116	1955	1955
52	4	56	1934	1930
60	7	98	1927	1926
71	4	57	1911	1920
87	6	68	1898	1883
91	7	77	1895	1882
123	9	130	1866	1862
165	6	72	1851	1855
174	4	57	1849	1850
189	13	132	1845	1845
203	7	81	1841	1844
209	6	72	1839	1838
227	6	71	1834	1834
231	6	69	1833	1833
246	8	88	1829	1830
254	6	75	1826	1824
287	22	370	1819	1820
295	5	65	1817	1817
299	5	61	1816	1814
314	7	74	1812	1811
323	7	74	1810	1809
331	7	76	1808	1808
351	3	50	1802	1805
359	9	78	1801	1799
381	11	88	1795	1795
434	6	69	1781	1784
536	4	57	1755	1753
550	6	67	1751	1751
563	6	68	1747	1747
583	7	77	1744	1741
712	17	120	1710	1711
729	11	95	1705	1709
770	16	127	1698	1699
778	16	119	1696	1697
795	16	111	1692	1692
819	13	104	1685	1684
829	16	113	1682	1682
839	13	96	1680	1677
856	8	84	1675	1674
869	26	137	1671	1671
879	10	93	1668	1663
901	12	98	1662	1658
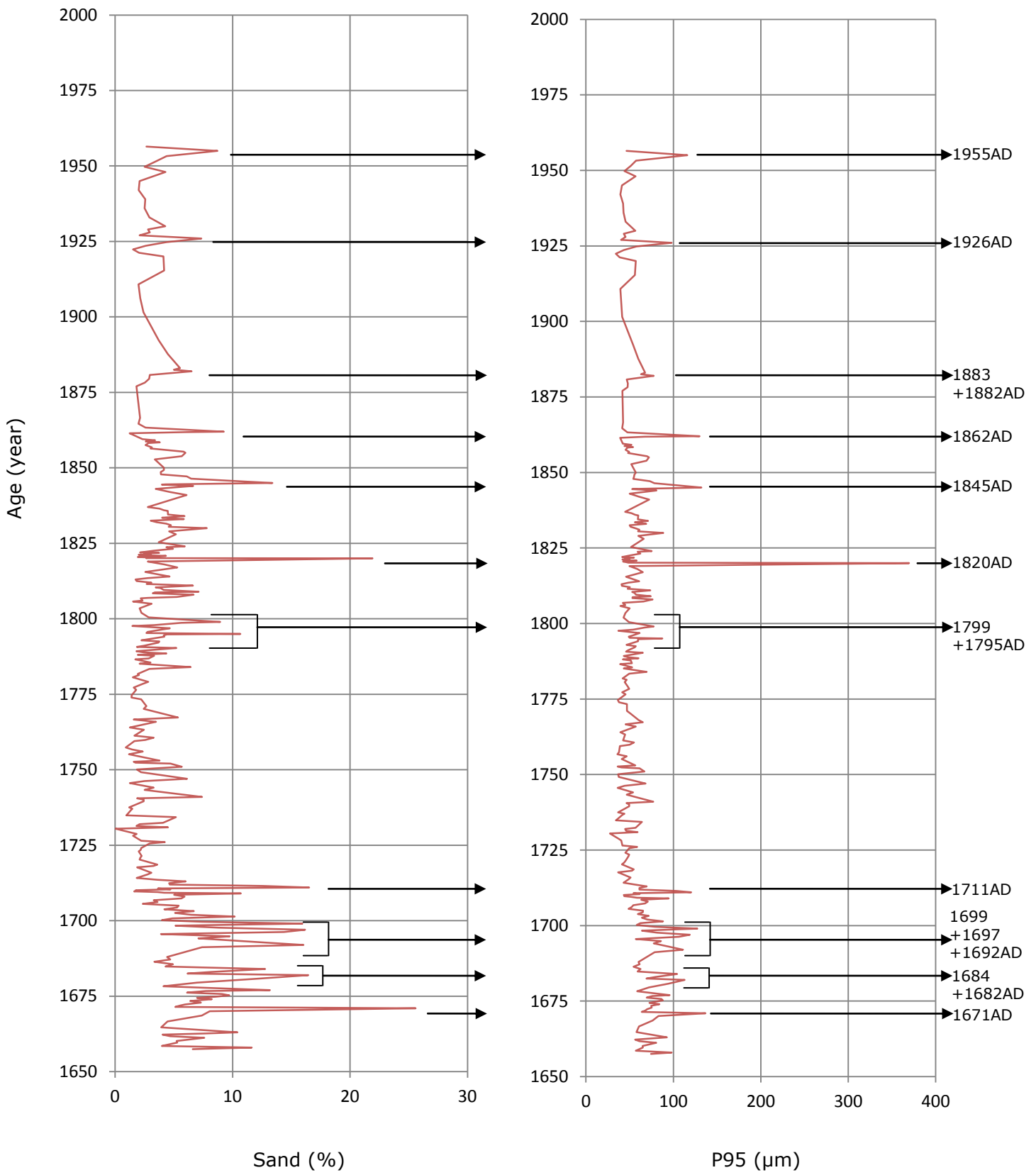
Figure 12: Zwarte Gat flood reconstruction sand percentage and P95

3.4	Flood magnitude comparison

In order to detect the same flood event in all three cores the three coring points need to be compared. Different sediment characteristics occurred at every location due to the impact of the flood and the composition of the sediment. To compare the locations, the P95 values have to be normalized.

The BAR sections 1 and 4 were not taken into account due to the influence of a sluice (section 1) and the coarser bottom core material (section 4). For every core the normalization of the P95 value was done in steps.

The deviation of all the P95 values in each section of the cores shows a trend (Table 10). The trend is an estimated development of the magnitude of a possibly occurring flood based on the P95/age correlations.

*Table 10: Trend coring section. *with P95 = P95 value*

Bienener Altrhein		
Section	**Depth (cm)**	**Trend (T)**
1	2-91	
2	93-151	T = -0.7934 (P95) + 184.66
3	153-842	T = -0.0093 (P95) + 57.432
4	844-849	
Rijnstrangen		
Section	**Depth (cm)**	**Trend (T)**
1	5-110	T = 3.0388 (P95) + 177.06
2	114-257	T = 0.4451 (P95) + 103.31
3	258-455	T = 0.006 (P95) + 97.374
4	457-475	T = 66.568 (P95) – 30516
Zwarte Gat		
Section	**Depth (cm)**	**Trend (T)**
1	30-253	T = 0.0583 (P95) + 49.164
2	254-453	T = -0.0848 (P95) + 86.384
3	456-693	T = 0.002 (P95) + 46.012
4	698-967	T = 0.066 (P95) + 20.64

The normalized value (N), between -3 and 9, for each lamination is calculated using the following formulas:

$$B = P95 \, / \, T$$

With T = Trend and P95 = P95 value

$$N = \frac{((B) - 1)}{\text{St. dev (B)}}$$

By plotting the three normalized P95 values together, the magnitude of the three locations can be compared. Figure 13 shows that at every location the magnitude slightly differs. A flood has a different impact on each location. Also the dating accuracy can have an influence on the positioning of peaks and troughs. Assumed is that the dating accuracy is optimized.

The figure shows two flood peaks in different time frames for every coring location as an example. The flood of 1926AD corresponds with a high peak for the Zwarte Gat. For the Bienener Altrhein on the other hand the peak is low which indicates a smaller P95 value and therefore a lower flood magnitude. The comparison shows a different height in magnitude for each year of an occurring flood. This can be explained due to the development of a flood along his path. A higher magnitude flood transports more and coarser sediment. Therefore at some locations the sediment differs.

Figure 13 also shows that the depth of the cores has a major influence on the correlations. The large number of peaks in a core refers to a deeper core section which gives a more detailed P95 value. For the Rijnstrangen a 475 cm core is taken in comparison with the 849 and 967 cm of the Bienener Altrhein and Zwarte Gat. Thus these both cores contain a higher resolution. As a consequence the correlations made with these values are more accurate.
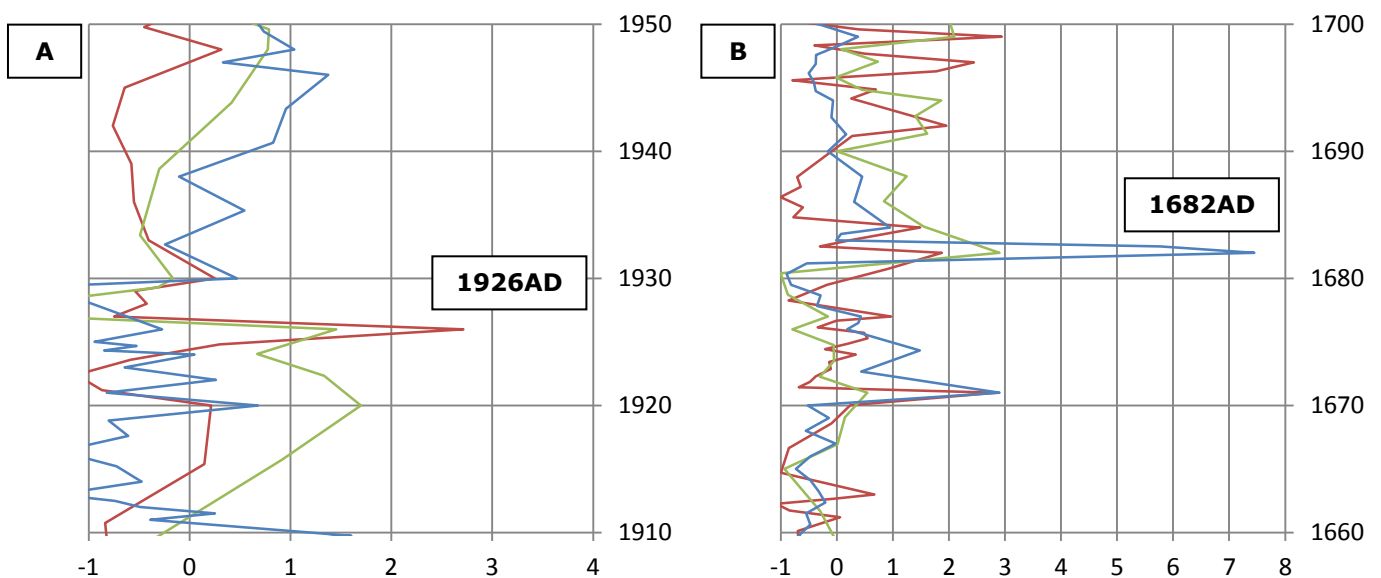
Figure 13: Combined normalization graphs for the Bienener Altrhein (blue), Rijnstrangen (green) and Zwarte Gat (red). [A = Period 1910AD-1950AD; B = Period 1660AD-1700AD]

36

The normalized peaks are checked fine tuned by comparing them to each location. This leads to an adjusted age depth curve. This age depth curve is shown in figure 9. The age depth curve is further fine-tuned by indicating the same pattern in the occurring peaks and correlating them with the class distribution of the historical floods (Table 6). For example: if a flood occurred in the normalized graphs at the Zwarte Gat and BAR core at 1700AD and at the Rijnstrangen a peak can be seen at 1699AD than the Rijnstrangen peak is fixed at 1700AD. By this method the more precise correlations are computed with the new normalized values for P95 (Fig. 15).
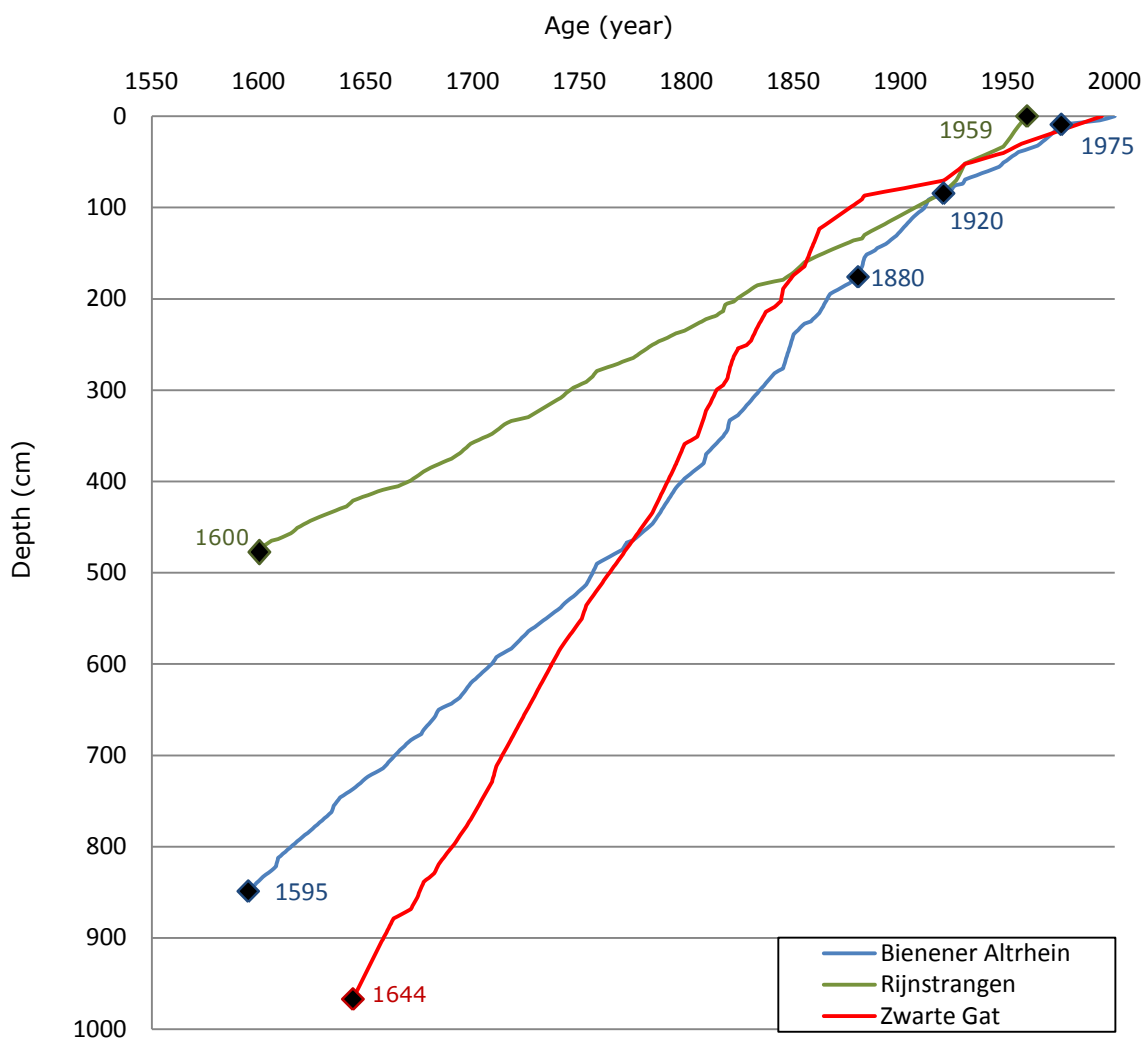
Figure 14: Adjusted age depth curves based on flood reconstructions with the new correlated adjustments due to the comparison of the normalized P95 records

Figure 14 shows both for the Bienener Altrhein and Rijnstrangen core a gradually linear increase of age further down the core. The Zwarte Gat core shows a rapid age deviation till 125 cm, 1862AD. After 125 cm the age increases more gradually further back in time

37

till the bottom at 1644AD. Compared to the first age depth curve made in 3.2 the age depth curves are more detailed.
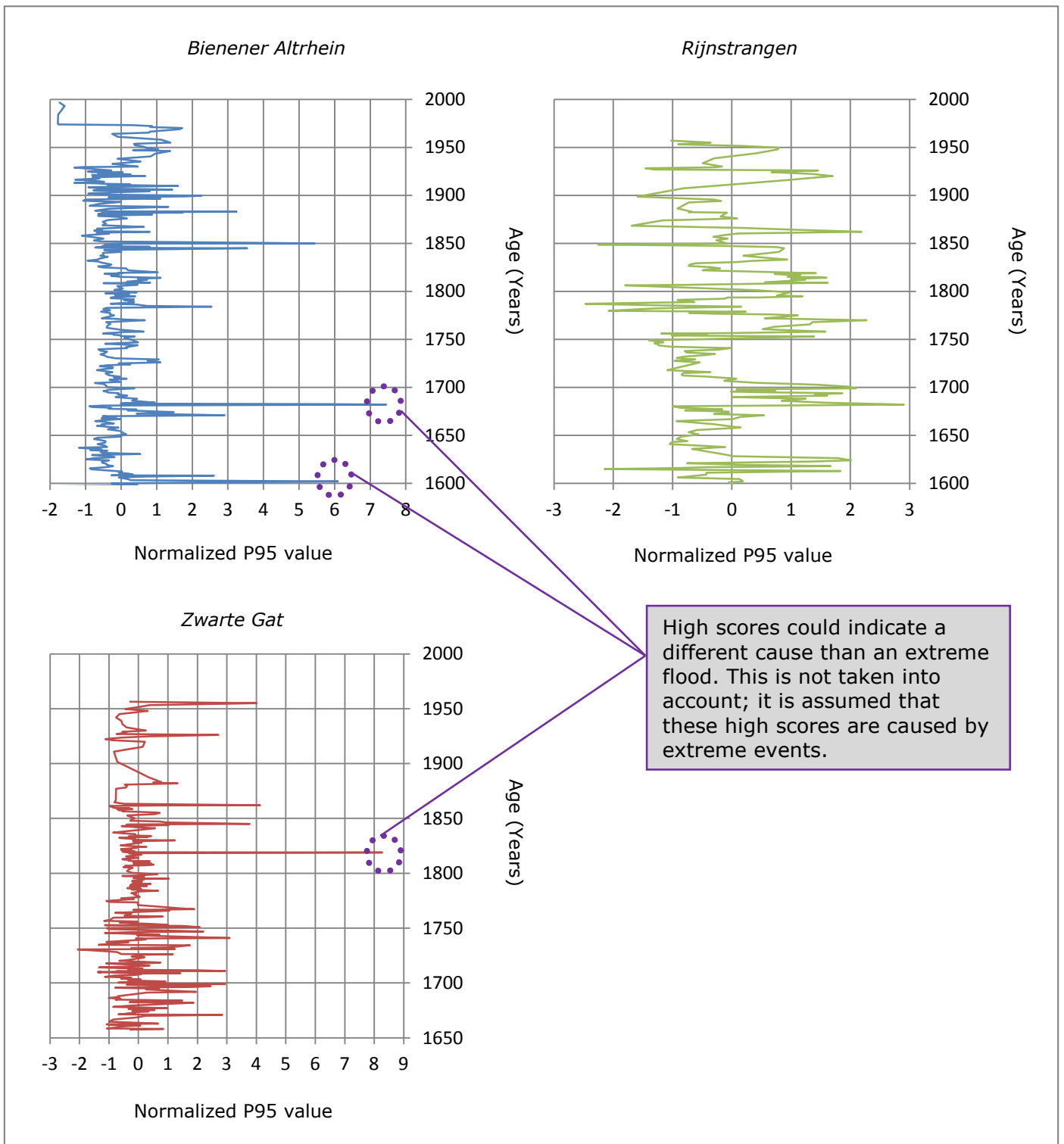
Figure 15: Normalization of the three coring locations

3.5	**Discharge estimations**

Defining discharges based on sediment layers was done by a correlation of the calibrated age/depth – P95 correlation against the Q known for 1817-2010AD. The correlated peaks in this period are determined for each location by plotting them into a graph to define the trend (App. 3). The trends contain an uncertainty which depends on the scattering of extreme values. The uncertainty is represented by a number R^2, the coefficient of determination, between 0 and 1 (1 is a perfect fit).

Bienener Altrhein: Q = 3619 ln (Pnorm) + 3487.9 R^2 = 0.33

Rijnstrangen: Q = 4512.9 ln (Pnorm) + 2883 R^2 = 0.32

Zwarte Gat: Q = 2609.5 ln (Pnorm) + 4912.7 R^2 = 0.24

With Q = Annual maximal discharge and Pnorm = Normalized annual P95 + 3

Before defining the trend to exclude negative numbers +3 is added to the normalized P95. Therefore by using this formula +3 needs to be added to the normalized P95 value.

The trend for the period 1817-2010AD is used for the extrapolation of the samples back to 1595AD (App. 4). The extrapolated values represent the average value over each samples width. By comparing the extrapolation to the converted Q Lobith per location, the following can be concluded (Fig. 16):

Bienener Altrhein

Overall the same patterns in trend and estimated discharge are observed. The extrapolation (red line) is closer to the converted Q Lobith 1817-2010AD. Maxima before 1817AD with an estimated discharge between 9600 m³/s and 12000 m³/s can be observed at 1784, 1682, 1671, 1608 and 1602AD. These floods had an impact with coarse material on the BAR location. Other floods that occurred are shown by peaks but with smaller sized sedimentation. Therefore they are difficult to indicate as a flood.

Rijnstrangen

The pattern of the plotted extrapolated discharge is more scattered in depth which corresponds with the converted Q Lobith. Fewer P95 values are present because of the depth of the core. The possibility of missing data is therefore more likely to occur in this core. The maxima before 1817AD occurring in 1814, 1809, 1799, 1795, 1770, 1758, 1753, 1699, 1694, 1682, 1624, 1618 and 1613AD all were around 10000 m³/s or more. Many floods are indicated using this method. The non-presence of floods can be caused

by the limited P95 values in the samples compared to the other two locations or due to the minor presence of course material at the coring location in time of the missing flood.

Zwarte Gat

The extrapolation is close to the converted Q Lobith 1817-2010AD discharge with some peaks that are similar at 1955, 1926, 1862, 1845 and 1819AD. With this similarity the outcome or extrapolation can be seen as a more accurate discharge indication. The range of the discharges is small due to the overall lower P95 values. Extremes before 1817AD are shown in a small range, 9300 m^3/s till 9650 m^3/s. They can be found at 1741, 1711, 1699, 1697 and 1671AD. These floods had a large impact at the ZG with sediment of a P95 value between 75-140 µm.

To compare the three locations the extremes are lined up with the known historical data (App. 1) that has been used in the correlation with their associated discharge (Table 7, 8 and 9). Table 11 shows correlated years in two or more cores and/or that have a known water level at Cologne are shown. As already been noticed at every location the flood discharge differs. In the last column the largest flood magnitude that occurs at the three cores is highlighted with an X.

All the 5 floods (bold) of the BAR core contain a P95 value of >100 µm. The largest P95 is at 1682AD with 208.63 µm. The RSTR core divides different P95 values. The first 4 flood (bold from 1814-1795AD) contain P95 values above 260 µm. This corresponds to section 2 in the core description. The other floods, 1770-1618AD in section 3, have a P95 value above 145 µm. The Zwarte Gat contains low P95 values. The flood of 1741AD located in section 3 is above 75 µm. The floods closer to the base of the core, 1644AD, all contained a particle size of 120 µm.

It is difficult to compare the three locations, as all locations yield different discharges. For instance some large flood magnitudes occur at the Bienener Altrhein but not at the Rijnstrangen or Zwarte Gat. The assumption is made that at a particular place the flood did not have the same magnitude or impact as at the other locations when the extrapolation does not show an extreme value.
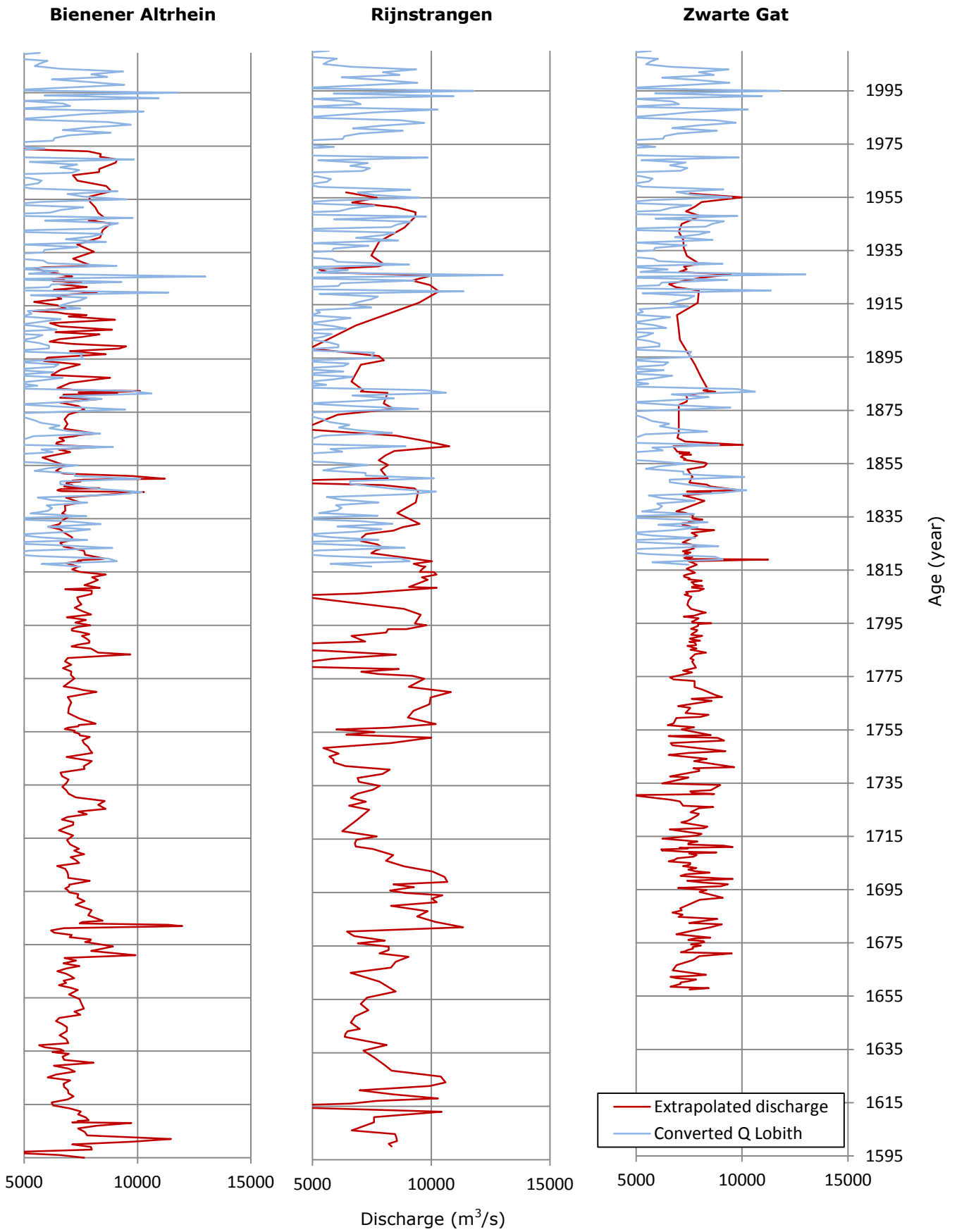
Figure 16: Plotted extrapolated discharge + the converted Q Lobith 1817-2010AD

Table 11: Extrapolated discharges of extreme known floods
* MF = Major flood and Q = discharge

Year	Bienener Altrhein (BAR)		Rijnstrangen (RSTR)		Zwarte Gat (ZG)		Converted Q Lobith (m³/s) (Toonen et al., in prep)	Waterlevel Colgne (m) (pegel Cologne)	Dike breaches (Buisman compilation)	Largest Q		
	Estimated discharge (m³/s)	P95 (µm)	Estimated discharge (m³/s)	P95 (µm)	Estimated discharge (m³/s)	P95 (µm)				BAR	RSTR	ZG
1814			**10190**	**293.07**	7779	60.95			6		X	
1809			**10210**	**296.88**	8127	74.14	9000	9.65	12		X	
1808					8192	76.30	8700	9.39	1			
1799			**9487**	**266.19**	8288	77.62			13		X	
1795			**9746**	**281.20**	8549	87.50			5		X	
1784	**9686**	**109.10**	8393	224.62	8304	69.41		13.63	22	X		
1770	8192	67.62	**10843**	**177.68**					1		X	
1758	8155	66.62	**10169**	**153.80**				10.10	1		X	
1753	7894	60.88	**9966**	**147.30**	8527	56.60		10.68	2		X	
1751					9152	66.99		9.73	3			
1747	7999	62.89			9217	68.26			7			X
1741	7662	56.08	8105	98.38	**9631**	**76.89**	9000	10.33	17			X
1729	8552	74.86						MF	8			
1726	8595	75.84						MF	13			
1711	7414	51.04			**9561**	**120.47**		MF	10			X
1709	7644	55.12	8264	102.11	8792	94.75		MF	7			X
1699	7892	59.67	**10683**	**172.62**	**9562**	**127.38**			4		X	
1697					9335	118.77			2			
1694	7384	50.12	**10459**	**164.61**					1		X	
1692					9089	111.13			1			
1684					8830	104.25			3			
1682	**11979**	**208.63**	**11385**	**200.93**	9047	112.95	10000	10.40	4	X		
1677			7884	94.17	8509	95.57		MF	3	X		
1674					8060	84.11			1			
1671	**9914**	**112.17**	8942	118.78	**9517**	**136.81**			2	X		
1663					8305	92.62		MF	2			
1658	7368	49.15	8374	105.00	**8426**	**98.10**	13000	11.98	10			X
1651	**7633**	**53.70**	7155	80.31			10000	10.28	14	X		
1644	**6890**	**41.41**	6765	73.66				MF	3	X		
1638	6952	42.26	7964	96.08				MF	6		X	
1635	6744	39.17						MF	5			
1634	6965	42.34						MF	4			
1624	7028	43.12	**10599**	**170.40**				MF	11		X	
1618	7180	45.39	**10258**	**158.41**					3		X	
1609	7847	56.75	7400	195.06				MF	3	X		
1608	**9729**	**103.31**						MF	2			
1602	**11477**	**174.38**	8436	969.56				MF	7	X		

The largest flood that occurs at both the BAR and RSTR with a discharge of more than 11300 m^3/s is the one at 1682AD. The ZG core shows a discharge of 9047 m^3/s which is much less. Therefore it is assumed that the flood of 1682AD had a larger impact at the Bienener Altrhein and the Rijnstrangen.

Other remarkable values in table 11 can be seen at 1651 and 1658AD. The three locations give no indication of an occurring flood. The flood data records instead show that there have been 10 or more dike breaches in both years. A water level of more than 10 meters in 1651AD and almost 12 meters in 1658AD at Cologne indicates an occurring flood. The extrapolation on the other hand shows no sign of an occurring flood. Reasons for the absence could be ice dams or nearby dike breaches that had a decreasing influence on the water level. Due to these diverse causes it can be concluded that at the three locations the occurred floods had no influence in the deposition of large grains size particle sedimentation. Compared to the results made by Winkels *(2011)* these floods did occur at the BAR location. The method is therefore not 100% solid, some floods are not indicated.

Another location based flood can be found at 1784AD for the Bienener Altrhein. With a water level of 13.63 meters and 22 dike breaches this flood only deposited coarse flood sediment at the Bienener Altrhein. The RSTR and ZG cores do not designate a flood. It is unlikely that the flood did not occur at the RSTR and ZG core. Again at these locations it can be concluded that floods were not detected by using the P95 method.

3.6	Flood frequency analysis

The annual maximum flow, obtained with the extrapolation was used to calculate the return period for each location. The return period is a measure of how often a flood of a given size is likely to occur. With equation 1 the return period (Rper) is calculated:

Equation 1 : $Rper = (n + 1) / M$

With
n = Number of years
M = Rank of the flood in the N year record

High magnitude floods have a lower frequency of occurrence than small magnitude floods. The flood magnitudes that occurred in the last 400 years differ in magnitude. By using a logarithmic scale to plot a graph the nonlinear data appears in a linear line and can be fitted with a logarithmic trend line (Fig. 17). The trend lines are based on the extreme discharges above 6700 m^3/s. Using the discharges lower than 6700 m^3/s would influence and overrate the extreme events and thus the trend.

Figure 17: Flood frequency plot (m^3/s) based on the converted Q Lobith (1817-2010AD) with the correlated sediment data for the Bienener Altrhein (1595-1816AD), Rijnstrangen (1658-1816AD) and Zwarte Gat (1600-1816AD)
With Q = Discharge (m^3/s) and Rper = Return period (years)

Rijnstrangen

$Q = 978{,}35 \ln (R_{per}) + 6590{,}8$

Zwarte Gat

$Q = 1215{,}9 \ln (R_{per}) + 6631{,}6$
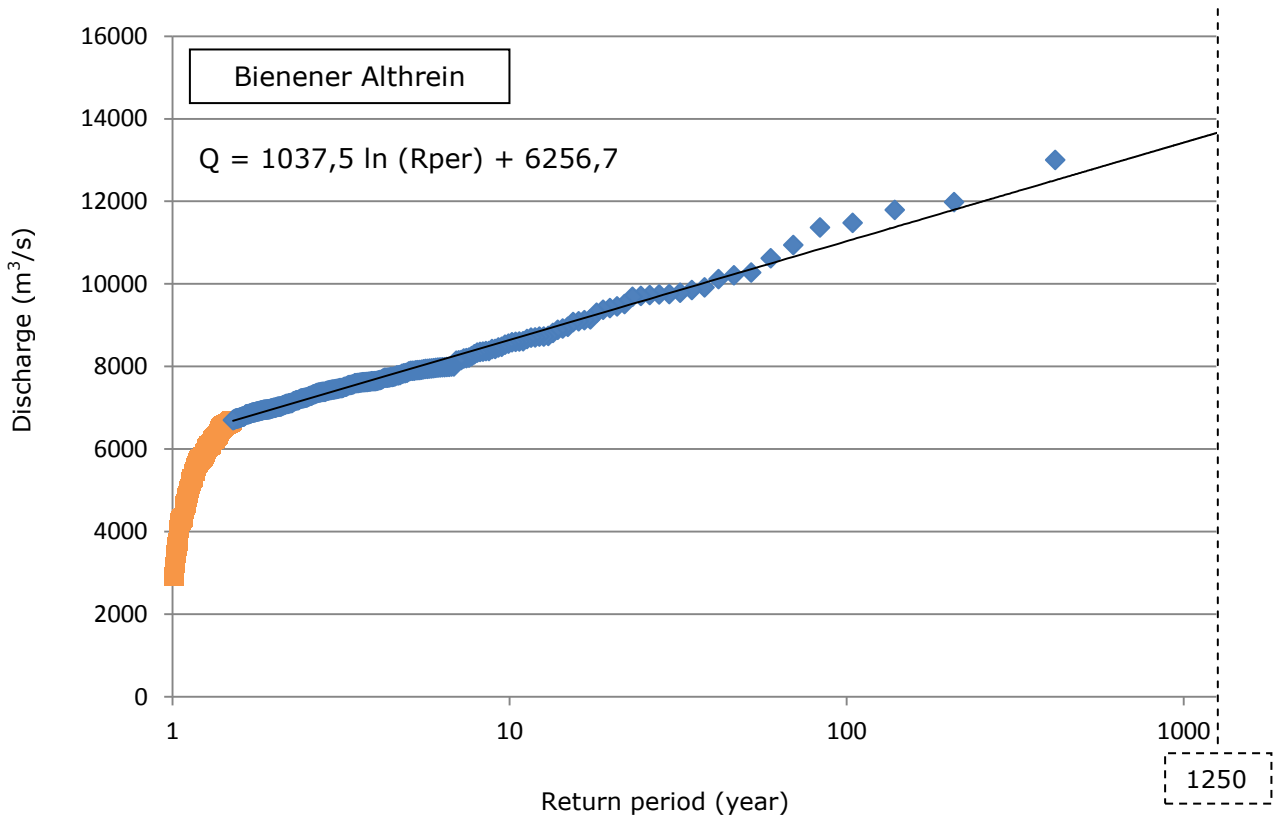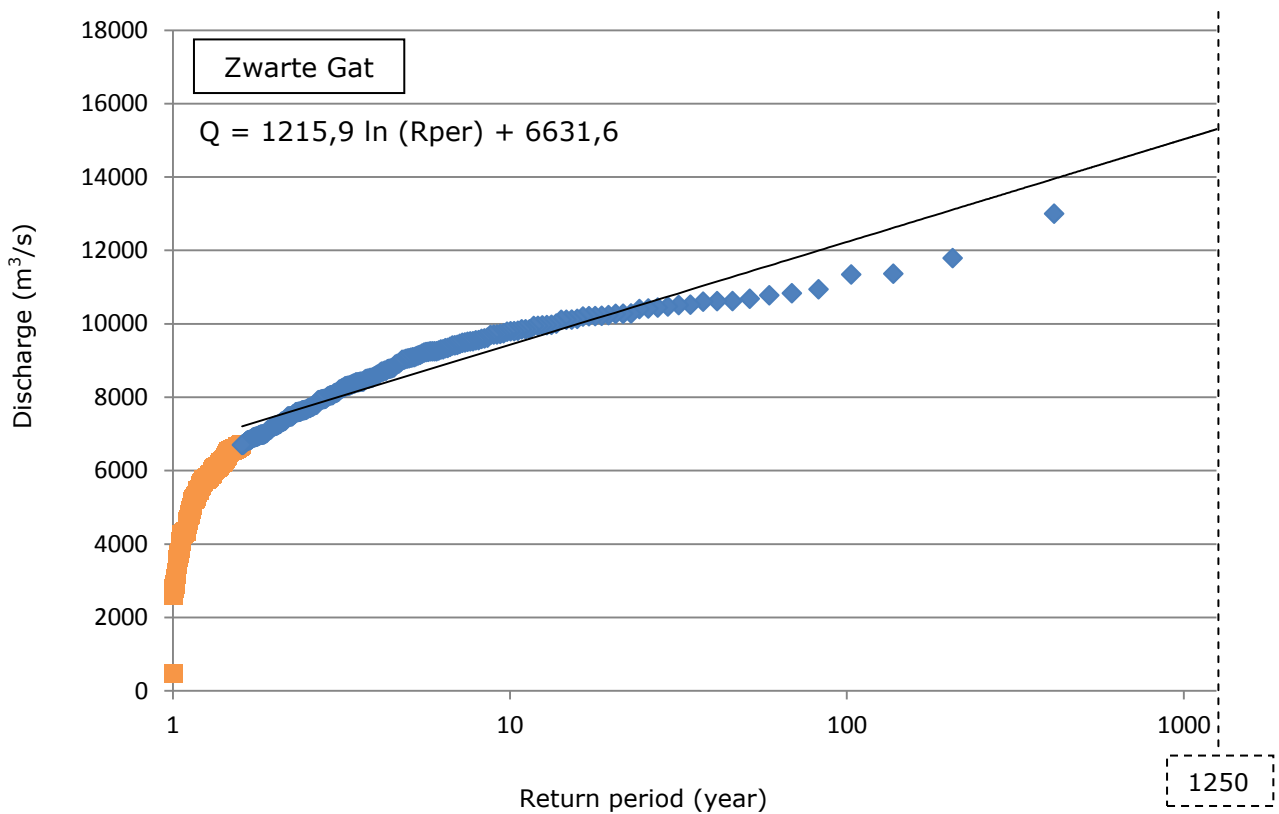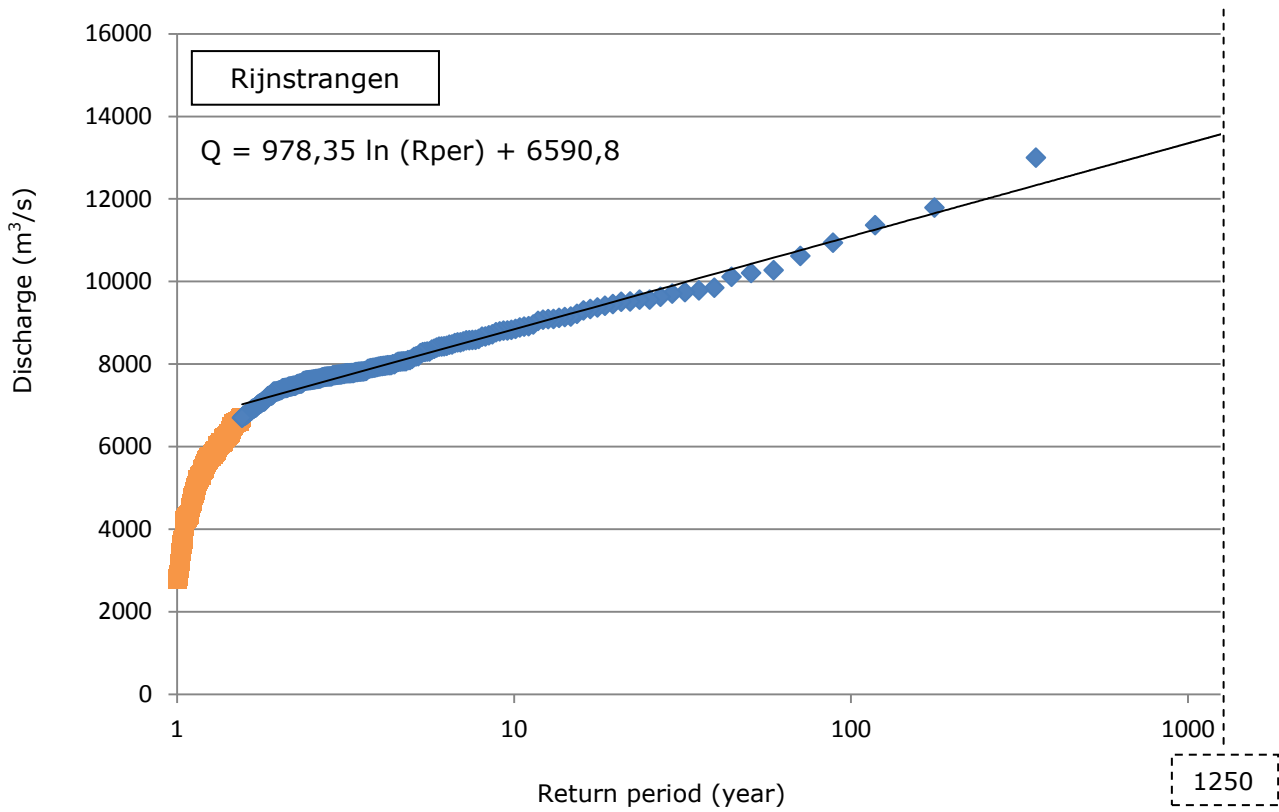
With these formulas the design discharge for different return periods can be calculated for each location based dataset (Table 12). The statistical uncertainty decreases by using a 400 year dataset instead of the approximately 100 year timeframe.

Table 12: Design discharge (m^3/s) for different return periods based on the converted Q Lobith (1817-2010AD) with the extrapolated data for: the Bienener Altrhein (1595-1816AD); the Rijnstrangen (1658-1816AD); the Zwarte Gat (1600-1816AD) and the extreme discharges which are the highest reconstructed discharge magnitudes that occurred at the three locations combined (1595-1816AD)

	Bienener Altrhein	Rijnstrangen	Zwarte Gat	Extreme discharges
Return Period	Design discharge (m^3/s)			
Once in				
10 years	8646	8844	9431	9576
100 years	11035	11096	12231	12193
1000 years	13423	13349	15031	14810
1250 years	**13655**	**13567**	**15302**	**15063**

The assumption was made that not all floods are found using the P95 method. This is due to different depositions of coarse material at the coring locations. To determine the maximum design discharge all floods with the maximum discharges indicated need to be used. Per year the maximum known discharges that occurred at one of the three locations are filtered to the extreme discharge situation.

The calculations of the design discharge (DD) for the three cores show that a 1250 year recurrence time flood has a discharge larger than 15000 m^3/s at the ZG core. Both the cores BAR and RSTR have a DD under 14000 m^3/s. With this knowledge the suggestion can be made that the Dutch government's decision to adjust the design discharge towards 2015AD into 16000 m^3/s is sufficient.

Figure 18 shows the maximum design discharge (black line) that is possible to occur in a given year based on the extreme flood magnitudes above 6700 m^3/s. This results in the presence of more extreme floods in the extrapolated discharge data set. The maximum design discharge based on these extreme floods is 15063 m^3/s for a once in 1250 year occurring flood (Table 11). This DD is less compared to the maximum design discharge, 16000 m^3/s, the Dutch government uses to determine their dikes safety.

Figure 18: Design discharge (m³/s) based on the converted Q Lobith (1817-2010AD) with the maximum extrapolated discharge data 1595-1816AD With Q = Discharge, Rper = Return period and DQ = Design discharge
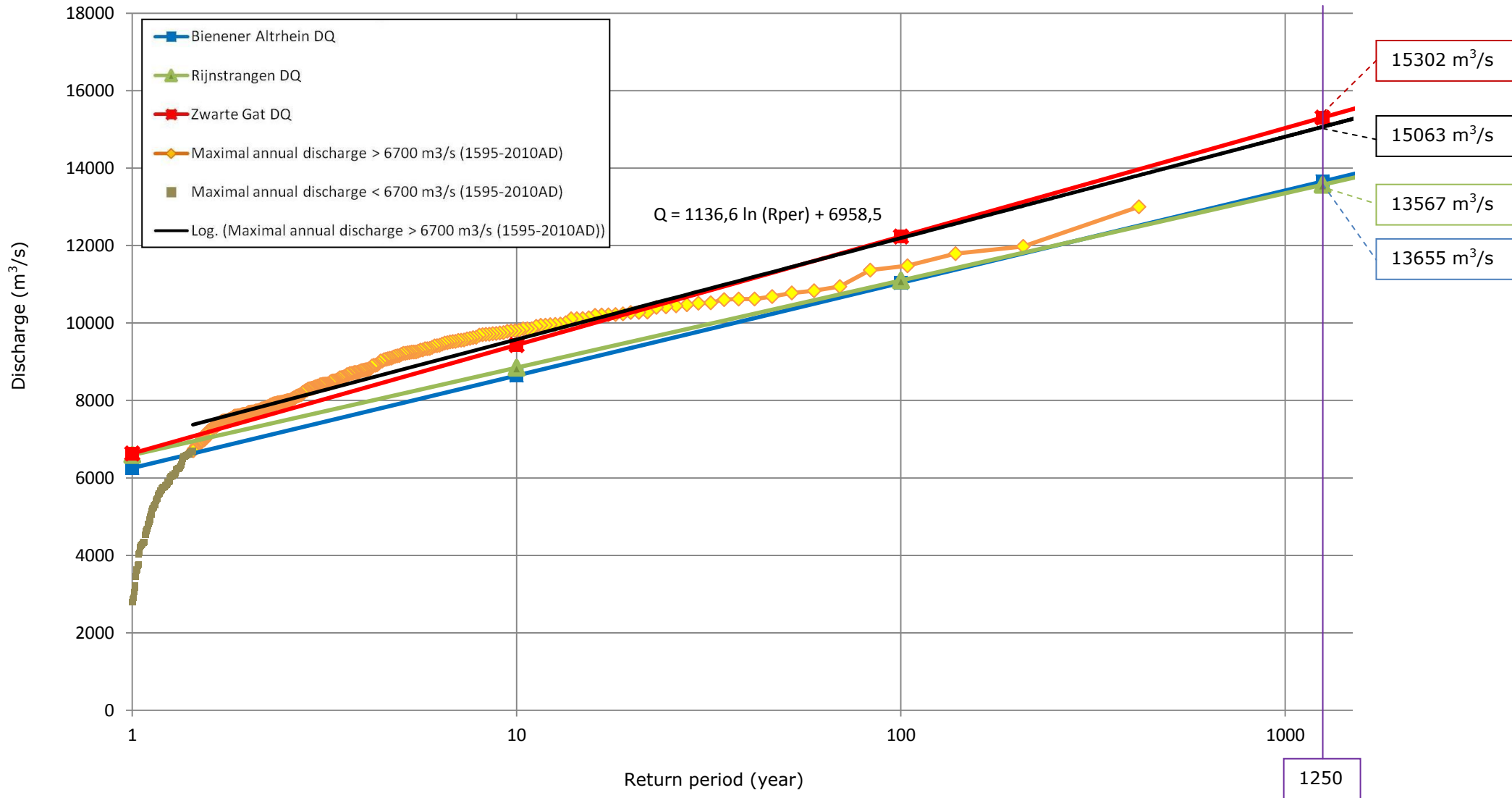
4	Discussion

A flood reconstruction which correlates the highest peaks of P95 values to the most extreme floods based on the age depth estimations is influenced by many factors. Not all factors have been taken into account. One is that the quality of dikes has improved. The older the age of a dike, the political or economic instability and with it his strength, the easier a dike breach can occur. Therefore it is well possible that recently (last 100 years) floods have to be of a higher magnitude to cause a dike breach. The number of dike breaches used in the classification is more indicative for large magnitude flood for the times before the dikes were strengthened. More dike breaches could have occurred if the dikes were not improved during time. More dike breaches would lead to an indication of a high magnitude flood which would be connected to a high P95 value and increase the flood indications. Also the down cutting of the present Rhine could have had an influence on the high sand percentages. The result of floods could be an influence on the river morphology. That is why during time the type of sediment and with it the discharge indication can differ with changing water levels. The assumption is made that this is not the case, but it has to be kept in mind. Dead wood is found in the samples. The presence of this material, which is removed during the analysis, could have an influence on the deposition of sediment. This influence is not taken into account.

Historical information helps to define an age-depth relationship for the sediment cores. The Zwarte Gat has the most historical information which leads to a bend in the age depth curve. The Bienener Altrhein and Rijnstrangen curve looks quite linear which is a result of the information available before starting the correlation. Expending and using more fixed points before starting the correlation will give a more precise age depth curve.

The flood comparison shows different normalized P95 values for the three coring locations. This means that one occurring flood has a different sedimentation impact on various locations. It can be questioned from which core the P95 value is indicative for the historical flood that occurred. The occurring peaks help to indicate the exact age of the extreme event. Due to the small amount of large grains in some parts of the cores not all floods occurred at the locations or they were not noticed and retrieved during the analysis. Analyzing more cores on different locations would help to determine the occurrence of historical floods.

The (trend) formula that is used to calculate the annual maximal discharge contains an uncertainty which depends on the scattering of extreme values. For both the BAR and RSTR core the R^2 value is around 0,3 and for the ZG 0,24. These values mean that the trend and therefore the calculated annual maximal discharges contain a large uncertainty. This uncertainty has to be kept in mind by checking the discharges outcome.

The comparison shows locations that give no indication of an occurring flood. The flood data records instead show that there have been 10 or more dike breaches. Reasons for the absence could be ice dams or nearby dike breaches that had a decreasing influence on the water level. Due to these diverse causes it has to be noticed that some floods are not indicated. Therefore several occurred floods had no influence in the deposition of large grains size particle sedimentation at these locations. The method is therefore not 100% solid.

During the flood frequency analysis the trend lines are based on the extreme discharges above 6700 m^3/s. This is done to undo the influence and overrating of extreme events due to the lower discharges than 6700 m^3/s. This discharge limit is estimated by comparing the three flood frequency plots in figure 12. The limit can be questioned because the exact point of extreme discharge events differs per frequency plot.

The extrapolation is based on the calibrated age-depth / P95 correlation against the correlated extreme events from 1817-2010AD. A small data set from 1817-2010AD to determine a once in 1250 year possible occurring flood gives a large statistical uncertainty. One specific extreme event has a very large impact on the discharge estimations. The extrapolation of these magnitudes till 1595AD gives a better estimation of the floods discharge. It has to be noticed that 400 years of data is still not fully representative for 1250 years, it reduces the statistical uncertainty.

Compared to the design discharge decided by the government the extreme scenario discharge of 15063 m^3/s is less but close to 16000 m^3/s. Flood data of around 200 years is expanded to approximately 400 years. More discharges are determined to extend the discharge data to calculate and minimize the uncertainty of the design discharge. As a consequence of the floods during the 200 years expansion it was expected to increase the design discharge which is not the case. No major extreme events occurred during the extended time frame that increased the discharge estimations.

Previous research describes the usability of the used data. Glaser and Stangl (2003) brought up some discussion points on how to use historical information towards floods. Historical information can be incomplete and are based on various types of sources which causes a large heterogeneity in the type and the quality of the historical records. Many documented flood disasters that occurred in the past were not caused by a very large discharge, but were also caused by neglected maintenance of the river dikes. Another cause of dike breaches was the formation of ice jams. Behind these jams the river water locally rises to very high levels, whilst discharge was only moderately high. During this study these other causes are not taken into account.

5	Conclusions

During this research the magnitude and frequencies of historical floods at three different locations along the river Rhine were reconstructed in order to extend the discharge records to minimize the uncertainty in the design discharge (based on the maximal annual discharges of the last 110 years). The studies objective was to expand the discharge data based on the sedimentation content, laminated in the soil of ponds and abandoned channels.

The presence of large grains in the deposited sedimentation could indicate an extreme discharge which suggests the presence of historical floods. The coring samples show peaks in sand- and P95 content (describes the size of the 95% largest particle in each sample). These extreme peaks have been correlated to the largest known floods.

Historical information was used to determine an age-depth curve. With flood correlation between the peak values in P95 with the known annual extreme discharge data the age-depth curve was further adjusted and fine tuned.

The P95 values differ among the 3 locations. Comparison of the locations was made by a normalization of these values. For every location the trend is determined to calculate the magnitude of the historical floods. The comparison results in different relative flood magnitudes at the same age in the three cores. The presence of an extreme flood depends on the location where the core has been taken. The most important cause is the difference in flood magnitude at the location which influences the P95 value of the sediment. Ice dams or nearby dike breaches could have had a decreasing influence on the water level.

The floods discharge at the Bienener Altrhein, the Rijnstrangen and the Zwarte Gat was calculated by extrapolating the correlation between the age of the extreme peaks and the converted discharge at Lobith (1817-2010AD). The extrapolated data for the period before 1817AD shows that the number of samples has an influence on the extrapolated result. For the Rijnstrangen the limited depth and therefore the smaller number of samples results in less precise correlations compared to the Bienener Altrhein and the Zwarte Gat.

In order to expand the knowledge towards the magnitude of historical floods this study shows that it is possible to identify historical floods in sedimentary layers in sediment fills of dike breach ponds and abandoned channels. The ~200 year discharge data set till 1817AD is expanded till 1595AD which results in a design discharge, which is based on a longer time series. With the assumption made, that not all floods occur on each location, the return period of the three cores and with them the most extreme discharge values are used to calculate the return period of the most extreme possible occurring flood scenario.

The design discharge calculated, based on the converted discharge at Lobith (1817-2010AD) and the most extreme magnitudes of the three extrapolated data sets, is 15063 m^3/s for a once in 1250 year occurring flood. The expansion of data shows no larger floods which would enlarge the design discharge with a recurrence time of 1250 years. The Dutch governments design discharge for the Rhine at Lobith is set at 16000 m^3/s. This study suggests that this design discharge used by policy is efficient.

6   References

Glaser, R., Stangl, H. (2003). Historical floods in the Dutch Rhine Delta. *Natural Hazards and Earth System Sciences 3*, pp. 605–613 European Geosciences Union.

Google earth (2011). URL: *earth.google.com*

Heiri, O., Lotter, AF., Lemcke, G. (2001). Loss on ignition as a method for estimating organic and carbonate content in sediments: reproducibility and comparability of results. *Journal of Paleolimnology 25*, pp. 101-110

Kleinhans MG., Cohen KM., Hoekstra J., IJmker JM. (2011) Evolution of a bifurcation in a meandering river with adjustable channel widths, Rhine delta apex, The Netherlands. *Earth Surface Processes and Landforms* 36 (15), pp. 2011-2027

Landschapsbeheer Gelderland (2010). Wielen receptenboek (digital publication). URL: *www.landschapsbeheergelderland.nl*

Middelkoop, H. (1997). *Embanked floodplains in the Netherlands*. *Geomorphological evolution over various time scales,* PhD thesis Utrecht University, NGS 224, pp. 341, The Netherlands.

Rijkswaterstaat Waterdienst (2003). Waterbase. URL: *www.waterbase.nl*

Steenhouwer, KJ., Hesselink, A., Beekmans, C., van der Zel, M. (2005) *Rijnstrangen rondom de hoofdkraan van Nederland; fietsen door twintig eeuwen waterstaatgeschiedenis.* RWS, RIZA, KROOS

Toonen, WHJ., Kleinhans, M., Cohen, K. (2011). Sedimentary architecture of abandoned channel fills. *Earth Surface Processes and Landforms,* Vol. 37, pp. 459-472

Toonen, WHJ., Winkels, TG., Prins, MA., de Groot, LV., Bunnik, FPM., Cohen, KM. (2012) A Lower Rhine flood chronology based on the sedimentary record of an abandoned channel fill. *EGU General Assembly Conference Abstracts 14*. 11596

Toonen, WHJ. et al., in prep. *Bayesian flood frequency analysis for the Lower Rhine.*

Van de Ven, GP. (1976). *Aan de wieg van Rijkswaterstaat*; wordingsgeschiedenis van het Pannerdensch Kanaal. Zutphen, De Walburg Pers.

Winkels, TG. (2011). *Flood reconstruction of sub-recent floods, based on the sedimentary record of the Bienener Altrhein*, BSc thesis dept. Physical Geography Utrecht University, pp. 33.

de Wit, M., Buiteveld, H., van Deursen, WPA. (2007). *Klimaatverandering en de afvoer van Rijn en Maas*, RIZA memo: WRR/2007-006, Arnhem, pp. 20.

Appendix 1

Table 13: Converted Q Lobith (Toonen et al., in prep), water level Cologne (pegel Cologne) and amount of dike breaches in the lower Rhine Valley & Delta (Buisman compilation)

Year	Converted Q Lobith	Waterlevel Köln (m)	Dike breaches	Year	Converted Q Lobith	Waterlevel Köln (m)	Dike breaches
2010	5692			1964	3061		
2009	4274			1963	5204		
2008	4351			1962	5774		
2007	6028			1961	5606		
2006	5675			1960	4765		
2005	5464			1959	5295		
2004	6611			1958	9120	9.13	
2003	9372	9.59	1	1957	6905		
2002	7958			1956	7610		
2001	8664			1955	9510	9.80	1
2000	6224			1954	5755		
1999	7920			1953	4280		
1998	9413	9.50	1	1952	7605		
1997	6926			1951	6620		
1996	4353			1950	6120		
1995	11790	10.69	1	1949	2790		
1994	5891			1948	9785	9.10	1
1993	10940	10.63	1	1947	5910		
1992	4917			1946	9140		
1991	6712			1945	8585		
1990	7028			1944	8295		
1989	4531			1943	3220		
1988	10274	9.95	1	1942	8475		
1987	7642			1941	7940		
1986	6194			1940	6835		
1985	4524			1939	8610		
1984	8697	9.10		1938	5000		
1983	9707	9.96	2	1937	7365		
1982	7931			1936	5895		
1981	6699			1935	5820		
1980	8811	9.30		1934	2905		
1979	6980			1933	4070		
1978	6336			1932	5820		
1977	6279			1931	6055		
1976	3459			1930	9075	9.15	
1975	4626			1929	4345		
1974	5904			1928	6490		
1973	3444			1927	5200		
1972	4931			1926	13000	10.69	4
1971	3633			1925	3745	9.80	
1970	9850	9.86	1	1924	9300		1
1969	5243			1923	6210		
1968	7334			1922	6090		
1967	6592			1921	2800		
1966	7422			1920	11365	10.58	2
1965	7108			1919	5295	9.62	

Year	Converted Q Lobith	Waterlevel Köln (m)	Dike breaches	Year	Converted Q Lobith	Waterlevel Köln (m)	Dike breaches
1918	7750			1868	6917		
1917	7475			1867	8351	9.08	
1916	6955			1866	5412		
1915	6550			1865	5051		
1914	7475			1864	4216		
1913	5150			1863	3721		
1912	5320			1862	8918	9.43	3
1911	4875			1861	5762		
1910	6605			1860	6257		
1909	5745			1859	4267		
1908	4815			1858	2906		
1907	5865			1857	3164		
1906	6420			1856	5680		
1905	3590			1855	7330		11
1904	5805			1854	6082		
1903	5460			1853	5453		2
1902	4815			1852	7227		
1901	5655			1851	7237		
1900	6092			1850	10114	10.23	2
1899	6092			1849	6587		
1898	4247			1848	6587		
1897	7598			1847	7546		
1896	7485			1846	8526		1
1895	7629			1845	10207	10.34	2
1894	4319			1844	8959	9.55	
1893	6515			1843	5597		
1892	6309			1842	6226		
1891	4319			1841	7784		
1890	6299			1840	5989		
1889	4329			1839	6226		
1888	6701			1838	6051		1
1887	5824			1837	5278		
1886	4669			1836	7742		
1885	5577			1835	3638		
1884	4247			1834	7021	9.11	
1883	9743	9.94	1	1833	8371	9.19	
1882	10619	10.52	1	1832	6041		
1881	6680	9.03		1831	7907		
1880	8423	9.13		1830	6783		1
1879	7186			1829	4628		1
1878	4680			1828	5762		
1877	6752			1827	7784		
1876	9454	9.75	1	1826	3762		
1875	6020		2	1825	6567		1
1874	2865			1824	8887	9.50	1
1873	5051			1823	5216		1
1872	5453			1822	4061		
1871	5732			1821	5556		
1870	6556			1820	8722	9.40	13
1869	6113			1819	9093	9.63	

Year	Converted Q Lobith	Waterlevel Köln (m)	Dike breaches	Year	Converted Q Lobith	Waterlevel Köln (m)	Dike breaches
1818	5762			1684			3
1817	7474			1682	10000	10.40	4
1814			6	1677		Major flood	3
1811			1	1674			1
1809	9000	9.65	12	1671			2
1808	8700	9.39	1	1665			1
1805			1	1663		Major flood	2
1799			13	1661			2
1795			5	1660			2
1784	13000	13.63	22	1659		Major flood	
1781			1	1658	13000	11.98	10
1776			1	1653		Major flood	
1775			2	1651	10000	10.28	14
1770			1	1646			1
1769			1	1644		Major flood	3
1764			1	1643		Major flood	2
1763			1	1638		Major flood	6
1761			1	1635		Major flood	5
1760			2	1634		Major flood	4
1758	9000	10.10	1	1633			3
1757			2	1628			1
1756			1	1625			1
1754			2	1624		Major flood	11
1753	10000	10.68	2	1622			2
1751	8500	9.73	3	1618			3
1749			2	1609		Major flood	3
1747			7	1608		Major flood	2
1744			5	1602		Major flood	7
1741	9000	10.33	17	1595	10000	10.54	25
1740			3				
1739			2				
1738			1				
1729		Major flood	8				
1728			2				
1726		Major flood	13				
1725			1				
1720			1				
1719			1				
1717			1				
1716			3				
1714			1				
1711		Major flood	10				
1709		Major flood	7				
1704			1				
1699			4				
1698			1				
1697			2				
1695			1				
1694			1				
1692			1				
1691			1				

Appendix 2

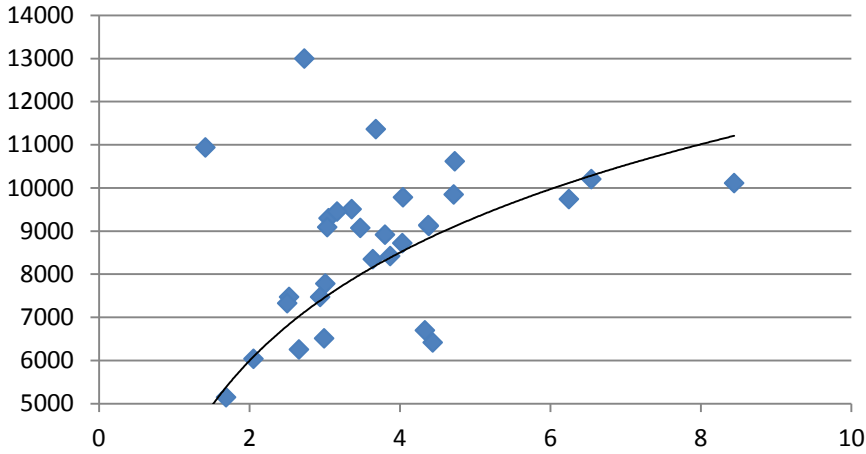*Figure 19: Q at Lobith m³/s 1817AD-2010AD (Toonen et. al, in prep)*
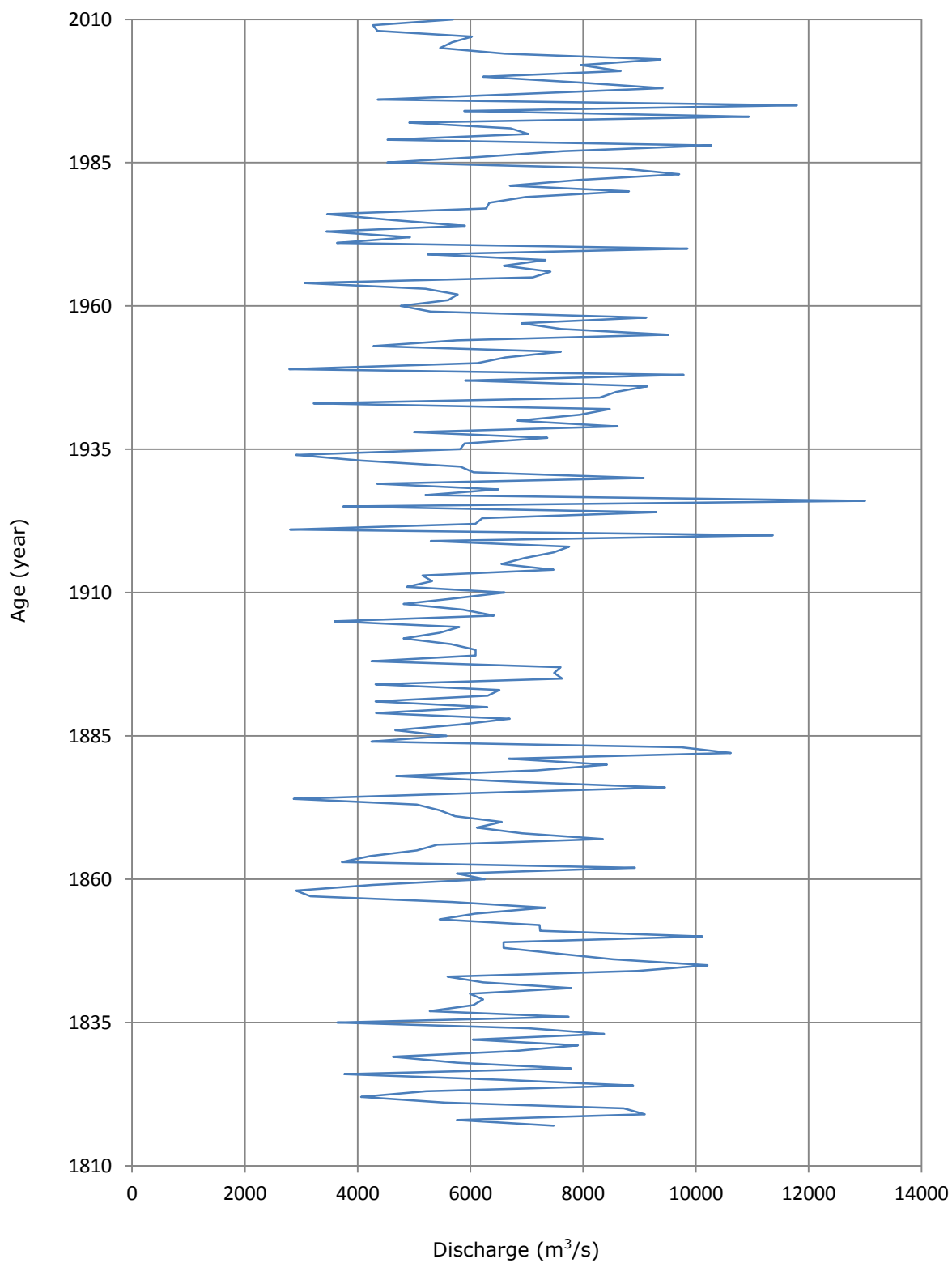
Appendix 3

Figure 20: Trend of correlated discharge with normalized P95 value for the period 1817-2010AD

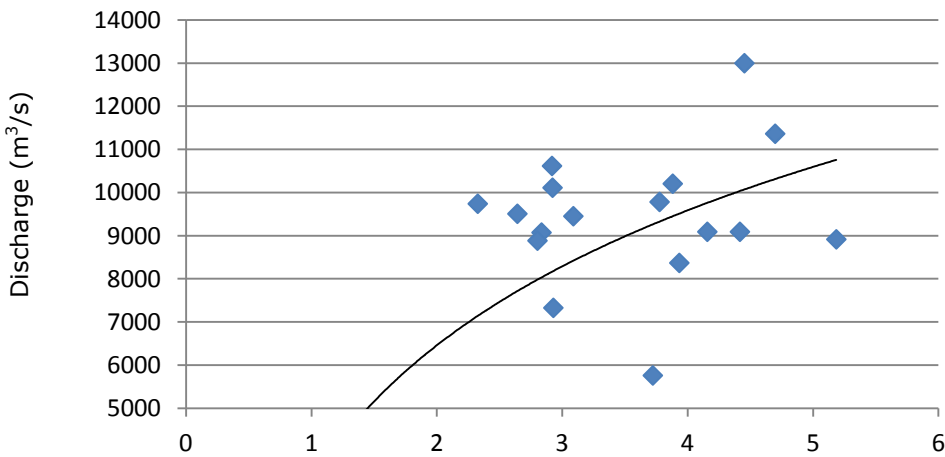
Bienener Altrhein

$$Q = 3619 \ln (Pnorm) + 3487,9$$
$$R^2 = 0,3274$$

Rijnstrangen
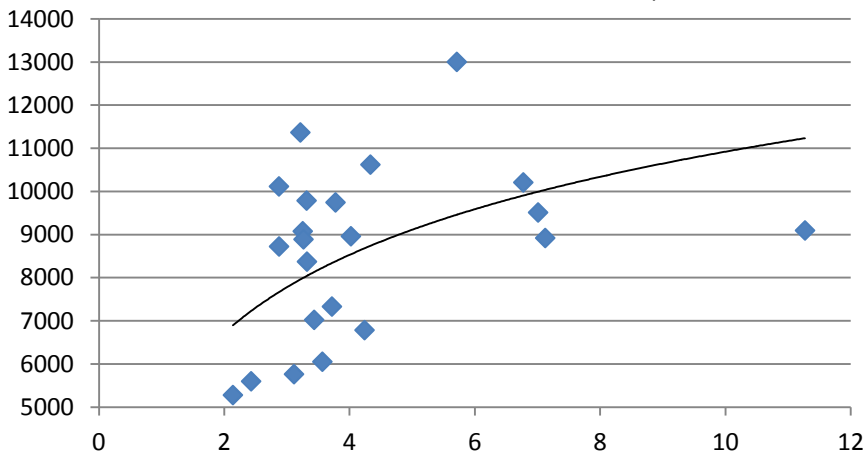
$$Q = 4512,9 \ln (Pnorm) + 3330,9$$
$$R^2 = 0,3156$$

Zwarte Gat

$$Q = 2609,5 \ln (Pnorm) + 4912,7$$
$$R^2 = 0,2353$$

Appendix 4

Figure 21: Estimated annual maxima at Lobith according to discharge for the Bienener Altrhein, Rijnstrangen and Zwarte Gat (1600-1817AD) based on the normalized trend of P95 content in sedimentation layers